

Guiding Protein Language Models with Reinforcement Learning

Filippo Stocco^{1,2}, Maria Artigues-Lleixà^{1,2}, Andrea Hunklinger^{2,3}, Talal Widatalla^{4,5}, Marc Güell^{1,6}, Noelia Ferruz^{2,1,*}

¹Department of Medicine and Life Sciences, Universitat Pompeu Fabra, Barcelona, Spain

²Centre for Genomic Regulation, the Barcelona Institute of Science and Technology, Dr Aiguader 88, Barcelona 08003, Spain

³Universitat de Barcelona, Facultat de Farmàcia i Ciències de l'Alimentació, Avda. Diagonal 643, Barcelona 08028, Spain

⁴Stanford University,

⁵Arc Institute

⁶ICREA, Institució Catalana de Recerca i Estudis Avançats, Barcelona, Spain

*E-mail: noelia.ferruz@crg.eu

Protein language models (pLMs) have demonstrated success at generating functional proteins across vast sequence spaces but lack the ability to design high-fitness variants on demand. Here, we iteratively guide pLMs toward user-defined objectives by applying reinforcement learning (RL). We demonstrate that RL can steer pLMs toward various protein properties, such as topologies or binding affinities, in a few iterations through long evolutionary trajectories. We apply our framework to the design of epidermal growth factor receptor (EGFR) binders, achieving a 26-fold increase in binding affinity in two iterations.

Protein language models (pLMs) have emerged as transformative tools for various applications, from structure prediction¹ to protein design². Recently, pLMs trained to generate proteins have shown promise in protein design, as demonstrated by the design of active enzymes from diverse families with less than 40% sequence identity³⁻⁵. While powerful, their sampling distribution mirrors common properties of the training data, limiting their ability to generate out-of-distribution high-fitness sequences⁶. We find that this limitation is intrinsic to pLMs and manifests across multiple metrics, including experimental enzymatic activities, sequence lengths, predicted pLDDT values, proportion of globular domains, or topologies (**Fig. S1a-e**). Similar constraints have been reported for other generative models recently⁷.

In recent years, reinforcement learning (RL) has met a wide range of success, with applications ranging from robotics⁸ to gaming⁹⁻¹¹ or autonomous driving¹². Grounded in psychological and neuroscientific studies of animal behavior¹³, RL allows models -agents- to learn and improve via trial-and-error by interacting with an environment that evaluates their actions. RL implementations, like Proximal Policy Optimization (PPO)¹⁴, Direct Preference Optimization (DPO)¹⁵, or Group Relative Policy Optimization (GRPO)¹⁶, are today's standard for iteratively aligning and pre-training¹⁷ autoregressive large language models (LLMs) like ChatGPT¹⁸ and Gemini¹⁹ to human preferences. Given the shared architecture and training objectives of pLMs and LLMs, we hypothesized that RL may allow the steering of pLMs by aligning them with user-defined properties. In particular, RL offers a framework to steer toward phenotypes of interest across long evolutionary trajectories.

Recent efforts applying RL in protein research have showcased the potential of the methodology for designing DNA and protein sequences²⁰, predicting thermostability²¹, the modelling binders²², aligning large pre-trained LLMs²³, or optimizing masked language models²⁴. This work's unique contribution is to optimize autoregressive pLMs through iterative

generation-testing cycles, in a similar manner to how LLMs like ChatGPT align with user feedback through RL. We hypothesize this approach should enable the optimization of user-defined properties while exploring considerably large sequence spaces. Our RL pipeline, ProtRL, is available at (<https://github.com/AI4PDLab/ProtRL>) and is directly applicable to any decoder-only pLM on HuggingFace, and further amenable to any differentiable method for protein design. In this study, we evaluate the performance of DPO across a range of in silico properties and explore the potential of using this method in the optimization of protein binders.

DPO optimizes models by maximally separating the log-likelihood of ranked ('good' vs. 'bad') sequence pairs (**Methods**):

$$L_{DPO}(\pi_{\theta}; \pi_{ref}) = -E_{(x, y_i, y_j) \sim D} \left[\log \sigma \left(\beta \log \frac{\pi_{\theta}(y_i|x)}{\pi_{ref}(y_i|x)} - \beta \log \frac{\pi_{\theta}(y_j|x)}{\pi_{ref}(y_j|x)} \right) \right] \quad (1)$$

Where π_{θ} is the model to be updated, π_{ref} the original model, β a constant to control divergence from the original model, and y_i, y_j the two ranked sequences (**Fig. 1a**). We further implement a DPO version that explicitly incorporates numerical rewards²¹, avoiding the need to define ranking pairs.

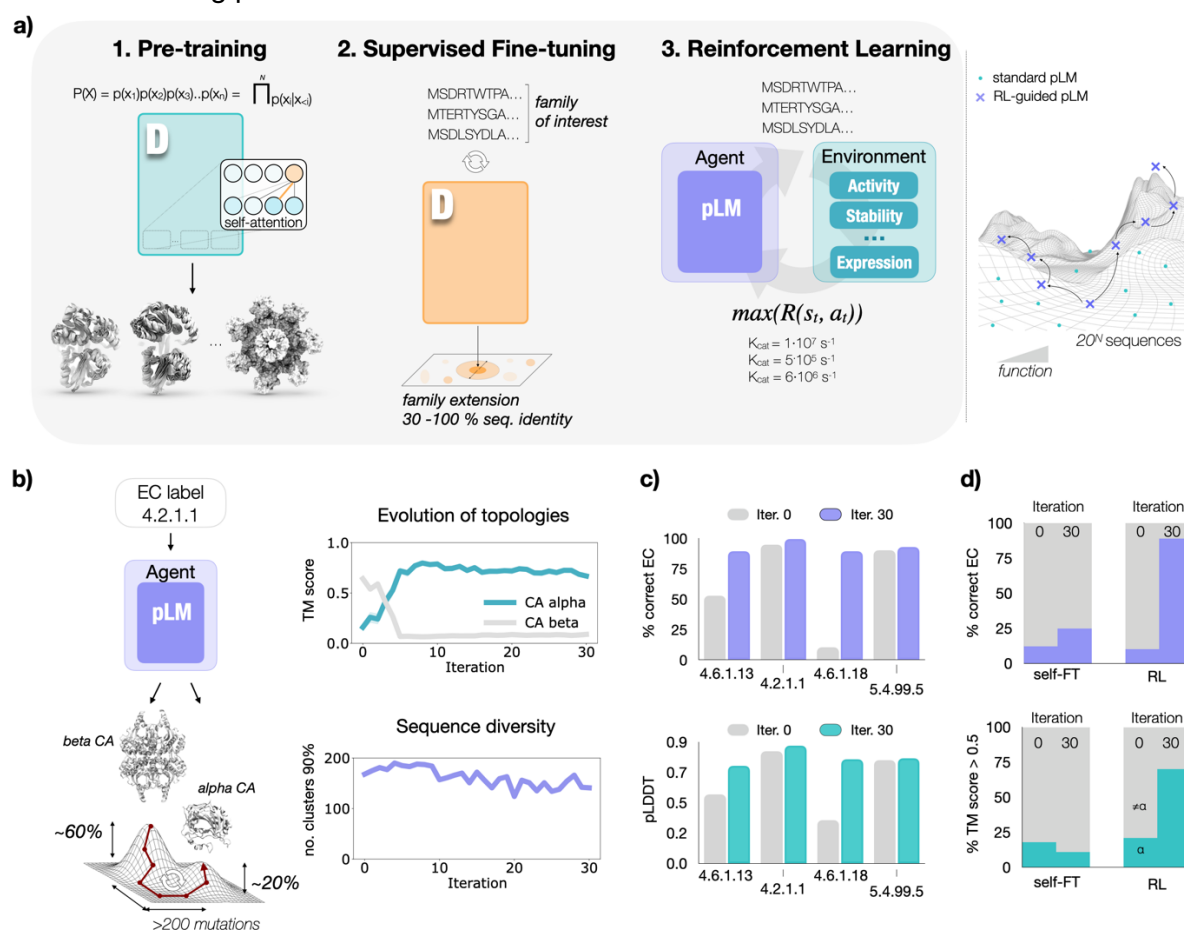


Figure 1: Overview of the RL pipeline for pLMs and optimization of in silico properties. (a) Models in this study are pre-trained with self-supervised causal modelling (pLMs publicly available), followed by supervised fine-tuning on narrower families, enabling the optimization of diverse properties through RL. This pipeline allows to traverse large phenotypic landscapes. (b) After pre-training, the pLMs sample from their training distribution, predominantly generating the most common traits, such as the most common carbonic anhydrases (CA) beta class. Through RL, pLMs shift their distribution toward other topologies on demand (alpha-CA, TM-score) while maintaining sequence diversity. (c) RL can steer the optimization of EC labels and pLDDT values, even for neighbouring families that are not specifically optimized. (d) Recursive fine-tuning (self-FT) alone fails to improve EC label prediction or topology after 30 iterations.

We first sought to optimize *in silico* properties, such as fold topology. In nature, there are 8 carbonic anhydrase (CA) subtypes with distinct folds (α , β , γ , δ , ζ , η , θ , and ι), and pLMs preferentially generate variants of the most common β subtype (**Fig. 1b**). We biased ZymCTRL⁴, a conditional pLM, towards generating α -CAs instead, for which we used a topological oracle (TM-score). TM-score values of 1 indicate an exact topology match, and values below 0.5 denote different folds. To avoid the pLM from maximizing the reward by generating increasingly longer sequences (a form of reward-hacking²⁵, **Fig. S2**), we introduced a length penalty in the reward function (see **Table S1** for explicit reward functions). After six iterations, over 95% of the sequences adopted the intended α subtype, with no dramatic decline in sequence quality or diversity (**Fig. 1b, Fig. S2**).

We next optimized protein function, as defined by CLEAN²⁶, a model that annotates sequences on their enzymatic commission (EC) numbers. Due to the scarcity of data for certain enzyme families, conditional pLMs fail to generate sequences for a given enzymatic class; i.e., when prompted with the EC label for pancreatic ribonuclease (EC 4.6.1.18), ZymCTRL would only generate sequences predicted with such function 10% of the time.

We rewarded the model considering the proportion of correctly labelled sequences, a length discount, and their pLDDT values. The model aligned to the objective function; in particular, 60% of the sequences were labelled as 4.6.1.18 after two iterations while improving their overall order as predicted by ESMfold (**Fig. S3**). Interestingly, we noticed that other EC labels (eg. 4.6.1.13) also improved their annotations and pLDDT predictions (**Fig. 1c**). These findings provide a general route for pLM optimization without requiring additional data.

We compared the performance of ProtRL against recursive fine-tuning. Supervised fine-tuning, the standard optimization technique for pLMs, optimizes pLMs by training them on smaller, focused datasets (**Fig. 1a**). We fine-tuned ZymCTRL iteratively on the best-performing generated sequences of the prior iteration, evaluated using the same reward functions as used in ProtRL for comparison. The recursively fine-tuned (self-FT) pLM failed to optimize properties after 30 iterations and it underwent collapse through the process, produced repetitive disordered sequences (**Fig. 1d, Fig. S4**).

Next, we aimed to optimize unbounded functions, i.e., continuous variables that can extend beyond training set limits. To this end, we implemented reward functions to maximize ESM1v²⁷ and ProteinMPNN²⁸ log-likelihoods (**Methods**), which have recently been shown to correlate with experimental outcomes in protein engineering campaigns²⁹. In both cases, we observed a consistent, maintained improvement, reflected by higher negative log-likelihood values (**Fig. 2a, Fig. S5**). We then used experimental data as a reward by training a supervised reward model with the dataset of α -amylases sourced from the Protein Engineering Tournament³⁰ that can predict the gain of activity versus the wild-type sequence (Specific Activity Performance Index, SAPI) for a design. On this occasion, the model was aligned by iteratively maximizing predicted enzymatic activities (**Fig. 2a, Fig. S6**).

We then focused on the experimental engineering of Epidermal Growth Factor Receptor (EGFR) binders. To this end, we first generated sequences from the pre-trained model (i.e., before any RL alignment) and experimentally tested the binding affinity of six designs (**Methods, Fig. 2b**). Round 1 yielded three binders with affinities of 328, 345, and 819 nM (**Fig. 2c, d; Table S2**). We then reinforced the model with these data and designed and tested candidates for round 2. Four out of nine surpassed the highest-affinity binder produced in the previous rounds, with dissociation constants (K_D) of 27.4 ± 4 nM, 181 ± 52 nM, 190 ± 49 nM, and 253 ± 32 nM. For reference, the wild-type EGF variant yielded a K_D of 759 nM in the same assay. Analysis of the successful binders further revealed correlation between *in silico* metrics and experimental fitness, providing a route to tailor reward functions in

subsequent rounds (**Fig. S7**). The optimization process explored diverse sequences. The tightest binder in the second round had a sequence identity of 80% to any known sequence (**Fig. S9**), and round 1, 2, showed decreasing average sequence identities of 88.6%, 73.1%. A generated round 3 with using these data yielded an average sequence identity of 63.9% (**Fig. 2e**), despite the models not being rewarded for increased diversity (**Table S1**).

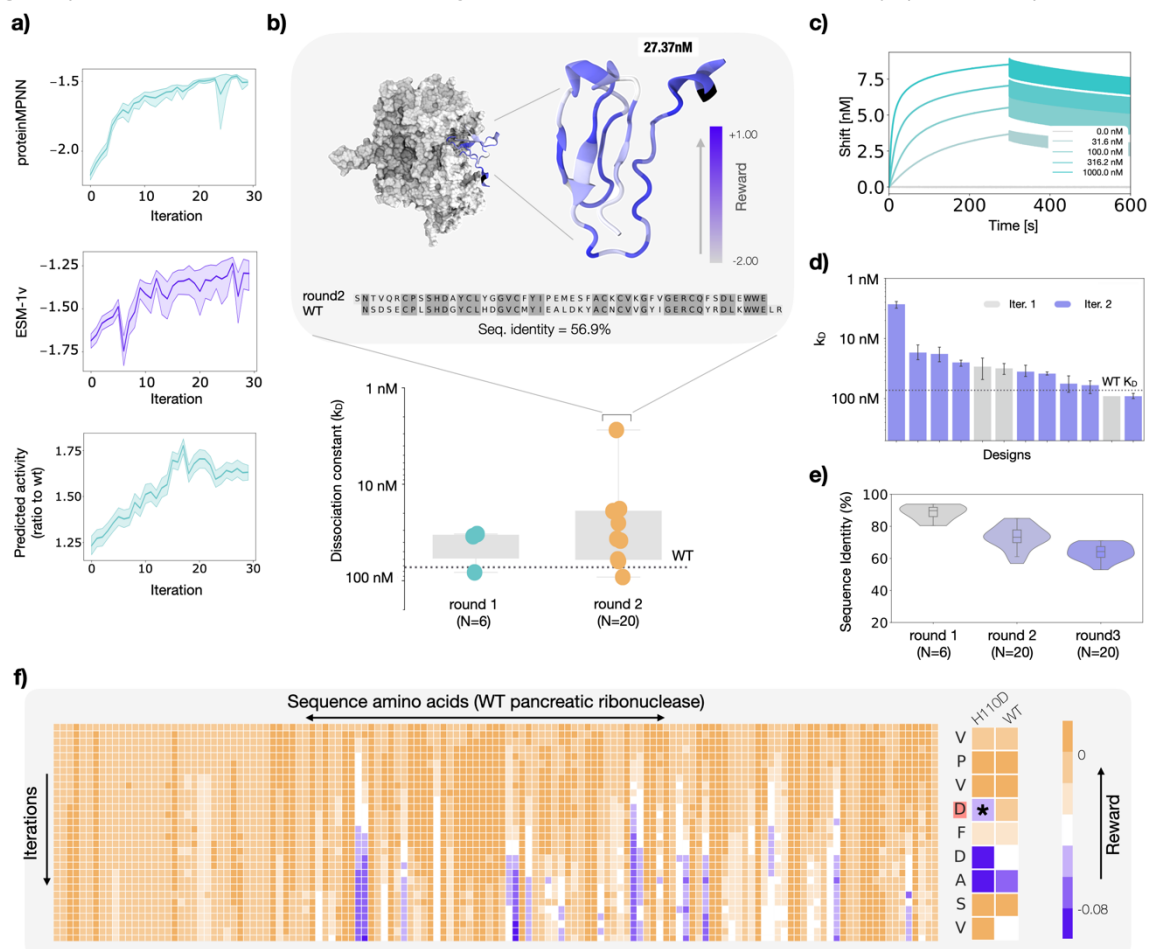


Figure 2: ProtRL optimization of unbounded functions and experimental binding affinities. **(a)** Optimization of ProteinMPNN and ESM-1v log-likelihoods (up, center), and predicted enzymatic activities (down). **(b)** Improvement of the affinity after two rounds of RL as determined by Bio-Layer interferometry (BLI), shown in logarithmic scale. Offset shows the AlphaFold2 prediction of the best binder in complex with EGFR. The two rounds are shown in y logarithm scale, inverting the K_D order for readability **(c)** Kinetic shift plots for the best binder. **(d)** Comparison of rounds and 2 in terms of binding affinity (log scale), and sequence identity **(e)**. **(f)** Token-level reward (r) computed for a ribonuclease sequence across the 30 ProtRL iterations ($\beta = 0.1$) (right). Detailed view of catalytic residues of the pancreatic ribonuclease (left). Mutation of the catalytic histidine at the C-terminal drops the reward locally without dramatically affecting the neighbourhood reward.

In addition to optimizing properties, DPO allows decoupling the reward into per-amino acid contributions³¹. This can be used to visualize the per-residue evolution of rewards during alignment (**Fig. 2f**, **Fig. S10**) or to identify critical residues upon mutation. Indeed, when mutating a catalytic amino acid, the CLEAN-aligned model (**Fig. 1c**) assigned a low reward (low likelihood) to that amino acid (**Fig. 2f**, **Fig. S10**). These findings offer a new route for interpreting the models' decision process and detecting crucial amino acids for a given oracle.

In conclusion, ProtRL introduces a generalizable framework for the design of high-fitness variants without explicit sequence identity or length constraints. By iteratively refining pLMs with the combination of external oracles, ProtRL can optimize complex external rewards, such as binding affinities. We envision incorporating ProtRL into automated laboratory settings where the experimental results constitute direct rewards, opening the door for intelligent agents that autonomously generate, test, and improve over time from experimental feedback.

Code Availability Statement

The code is available under the MIT license at <https://github.com/AI4PDLab/ProtRL>. The pLM used in this work is available at <https://huggingface.co/AI4PD/ZymCTRL>.

Data Availability Statement

The data used to run the experiments is available under the MIT license at <https://github.com/AI4PDLab/ProtRL>. The data to train the pLM ZymCTRL is available at <https://huggingface.co/datasets/AI4PD/ZymCTRL>.

Acknowledgments

We are grateful to Michele Garibbó, Michael Heinzinger, Maurice Brenner, and Alex Vicente for their insightful discussions. We thank Emyr James and the CRG IT team for support in using the CRG GPU cluster. We are most grateful to Adaptyv Bio, for testing our EGFR binders in their protein characterization platform as part of the Adaptyv Bio Protein Design Competition Round 2, and Julian Englert for assistance. We acknowledge Dana Cortade and Dave Estell for help interpreting the experimental α -amylase data, and the Protein Engineering Tournament for kindly testing our α -amylase sequences. We acknowledge the support of the Spanish Ministry of Science and Innovation through the Centro de Excelencia Severo Ochoa (CEX2020-001049-S, MCIN/AEI /10.13039/501100011033), and the Generalitat de Catalunya through the CERCA program. N.F. acknowledges support from a Ramón y Cajal contract RYC2021-034367-I funded by MCIN/AEI/10.13039/501100011033 and by the European Union NextGenerationEU/PRTR. M.A.L. acknowledges support from an FI Fellowship (AGAUR-Catalan Government) co-funded by the European Social Fund (Award 2024 FI-3 00065). We acknowledge support from the ERC-2024-Starting grant ATHENA (GA: 101165231). This project has received funding from the European Union's Horizon Europe under grant agreement No 101120466 (MSCA-DN supporting A.H.). Views and opinions expressed are however, those of the author(s) only and do not necessarily reflect those of the European Union. Neither the European Union nor the granting authority can be held responsible for them.

Conflict of interest

The authors declare no conflict of interest.

Methods

Direct Preference Optimization

From the original formulation of DPO, the loss (L_{DPO}) to be minimized is formulated as follows:

$$L_{DPO}(\pi_\theta; \pi_{ref}) = -E_{(x, y_w, y_l) \sim D} \left[\log \sigma \left(\beta \log \frac{\pi_\theta(x)}{\pi_{ref}(x)} - \beta \log \frac{\pi_\theta(x)}{\pi_{ref}(x)} \right) \right] \quad (3)$$

where π_θ is the policy to be updated, π_{ref} the original frozen model, β rules how much the model will drift from the reference, and y_w and y_l the selected and the rejected options for each pair comparison. In a recent contribution by Widatalla et al., 2024, two additional loss functions have been introduced: the ranked and weighted form.

Ranked Loss:

$$L_{DPO_{ranked}}(\pi_\theta; \pi_{ref}) = -E_D \sum_{k=1}^K \left[\beta \log \frac{\pi_\theta(x)}{\pi_{ref}(x)} - \log \sum_{j=k}^K \exp \left(\beta \log \frac{\pi_\theta(x)}{\pi_{ref}(x)} \right) \right] \quad (4)$$

Weighted loss:

$$L_{DPO_{weighted}}(\pi_\theta; \pi_{ref}) = -E_D \sum_{k=1}^K w^k \left[\beta \log \frac{\pi_\theta(x)}{\pi_{ref}(x)} - \log \sum_{j=k}^K \exp \left(\beta \log \frac{\pi_\theta(x)}{\pi_{ref}(x)} \right) \right] \quad (5)$$

Which, in other words, is the cross entropy of the ratio $r = \beta \log \frac{\pi_\theta(x)}{\pi_{ref}(x)}$ and the weight value w . The hyperparameter β determines how far the model should drift from the original probability distribution π . SoftMax has been applied to the weights w , on the batch dimension. The pytorch function `F.cross_entropy` has been applied to the ratio and the weights.

Intrinsic reward:

Intrinsic reward has been computed as in Rafailov et al.³¹

$$r = \beta \log \frac{\pi_\theta(x)}{\pi_{ref}(x)}$$

With $\beta = 0.1$ for Fig. 2b and 0.01 for Fig. 2f. In this case the log likelihood was computed per token.

Self-fine-tuning

s-FT involves iterative refinement of ZymCTRL by leveraging the top-scoring sequences generated at each iteration, as evaluated by a predefined scoring function $f(seq)$. The pipeline follows three sequential steps: 1) generate 2,000 synthetic sequences from ZymCTRL, 2) rank these sequences based on $f(seq)$ and 3) fine-tune the model using the top 200 candidates. This process iterates for 30 iterations. Triplicates of the training were carried out to increase the statistical significance of the results obtained.

Model training and generation

During s-FT, we retrained ZymCTRL with the Huggingface transformer's Trainer class, loaded from Hugging Face's transformers API (version 4.45.2). The fine-tuning was performed with a training and evaluation batch size of 4 and 1 with a learning rate of 8×10^{-6} . For every 10 steps, the model was evaluated and saved. The process was carried out for 25 epochs each iteration. The model with the lowest evaluation loss was chosen as the input for the next iteration. In all cases (ProtRL and s-FT) we generated using as inference parameters `top_k=9`, `top_p=1`, `repetition_penalty=1.2`, and `do_sampling=True`.

Structural Similarity: TM Score and Sequence Identity

Generated sequences were folded using ESMFold¹ loaded from Hugging Face's transformers API (version 4.45.2), and the resulting PDB structures were superimposed onto the wild-type structures from the Protein Data Bank using Foldseek³² (release 9-427df8a). Sequence identity was computed by aligning generated sequences to the training set of each updated ZymCTRL's model using MMseqs2 (Release 15-6f452).

Functional Annotation: CLEAN Class Enzyme Prediction and Cosine Similarity

Protein embeddings were derived using ESM1b³³, yielding matrices of size $L \times dim$ (where L is the protein length and dim is the embedding dimensionality). These embeddings were inferred into CLEAN's optimized embedding space (v1.0.1) to compute the cosine similarity between the studied sequence and the center of the latent space cluster corresponding to the target EC number.

Statistical Metrics: ESM1v and ProteinMPNN

ProteinMPNN score was retrieved using the "score_only" flag of ProteinMPNN GitHub repository (v1.0.1) and multiplied by -1 to be maximized with DPO as other features. ESM1v score is the average of the log probabilities of amino acids at each sequence position and was computed without masking relying on the previously established methods of sampling²⁹.

Activity prediction: training of regression models

Two classification models were trained following the notebook in Schmirler et. al 2024³⁴. The models utilized were ESM2 and ESM1v, in both cases with LoRA adapters. The two predicted activity by the two models has been averaged and used as reward ZymCTRL. We used the publicly available at the Protein Engineering Tournament GitHub repository³². The dataset comprises sequences paired with their respective Specific Activity Performance Index (SAPI), which represents the ratio of the specific activity of a variant to that of the reference. Specific activity is defined as the ratio of activity to the measured protein concentration. To enhance data quality, entries with no activity or expression values below 0.5 were excluded. The models were trained for 57 epochs using an 80/20 split for training and validation. A batch size of 4 and a learning rate of 3×10^{-4} were applied during training. Learning curves and Spearman correlations are illustrated in Fig. S6.

Fine Tuning of ZymCTRL and Reinforcement Campaign: EGFR binders design

ZymCTRL was fine-tuned using 600 sequences retrieved via BLAST, with the wild-type epidermal growth factor as the query. The label 4.6.1.18 was employed for annotation. Fine-tuning was conducted with a learning rate of 8×10^{-6} over 100 epochs. From the fine-tuned model, 20 sequences were generated and subsequently folded using AlphaFold Colab^{58,59}. Folding was performed with a single model, three recycles, and in single-sequence mode, utilizing the alphafold2_multimer_v3 mode. Model alignment was carried using ranked version of DPO and using all the binders from Adaptiv Bio competition 1 and 2. Binders were filtered based on TM score > 0.4 of the WT EGF and the reward was set as a sum of the Kd value, length and tm score itself as stated in Table S1. In round 1, 10k sequences were generated from the FT model and filtered them based on perplexity and length (greater than 49) to select the best candidates to be tested. In round 2, we applied two rounds of reinforcement learning (RL) using the same scoring function but with 10 and 20 epochs. For each run, we generated 10k sequences, ranked them based on perplexity, plddt, and pMPNN, and selected the top 20 sequences for testing. Similar to the previous rounds, in round 3 we aligned the selected sequences with 10 and 20 epochs of the previous experimental data points. The score also considered the expressibility of the sequences, as stated in table S1. The observed correlation between Kd and in silico metrics was used to score, filter (20k sequences), and select the binders for testing (20). Results of round 1 and 2 are publicly available in

https://github.com/adaptyvbio/egfr_competition_2 and <https://github.com/AI4PDLab/ProtRL> respectively.

In silico evolution of CD80 binders:

A multiobjective function was formulated using the correlation observed from round 2 results and the metrics employed in BindCraft [ref]. Over iterations, the overall score improved. Detailed loss function in Table S3.

Binders analysis:

Results from round 1 and 2 were analysed using in silico metrics, and a correlation matrix was computed. In silico metrics were computed as previously described [bindcraft]. Correlation was carried only in designs with measured K_d value. Sequence alignment was performed using the online tool BLAST with default settings and only one result per query (the highest value of sequence identity found). The intrinsic reward score was calculated as the ratio of the log likelihood per token of the aligned model with the pre-trained model (AI4PD/ZymCTRL) multiplied by beta, as per equation 6. The obtained intrinsic reward was used to color code the structure.

Affinity characterization:

K_D, k_{on}, and k_{off} were calculated by using Adaptyv's automated expression and affinity measurement using Bio-Layer Interferometry (BLI)³⁵. The protocol starts with a DNA optimization step to ensure adequate expression of all sequences, followed by a cell-free expression protocol, and BLI for measuring binding affinity. The replicates correspond to different samples (expression). The target protein, in this case EGFR, is introduced at different concentrations to measure both the weak and strong interactions to the immobilized binder.

Training and evaluation:

Training was conducted on a GPU H100 for each task, ranging from a few GPU hours to one day of training to reach the 30 iterations for DPO and several days per experiment for s-FT. In all cases, unless explicitly reported in the main text, the hyperparameters for DPO are stated in **Table S3**.

References

1. Lin, Z., Akin, H., Rao, R., Hie, B., Zhu, Z., Lu, W., dos Santos Costa, A., Fazel-Zarandi, M., Sercu, T., Candido, S. & Rives, A. Language models of protein sequences at the scale of evolution enable accurate structure prediction. *bioRxiv* 2022.07.20.500902 (2022). doi:10.1101/2022.07.20.500902
2. Ruffolo, J. A. & Madani, A. Designing proteins with language models. *Nat. Biotechnol.* **42**, 200–202 (2024).
3. Romero-Romero, S., Braun, A. E., Kossendey, T., Ferruz, N., Schmidt, S. & Höcker, B. De novo design of triosephosphate isomerases using generative language models. *bioRxiv* (2024). doi:10.1101/2024.11.10.622869
4. Munsamy, G., Illanes-Vicioso, R., Funcillo, S., Nakou, I. T., Lindner, S., Ayres, G., Sheehan, L. S., Moss, S., Eckhard, U., Lorenz, P. & Ferruz, N. Conditional language models enable the efficient design of proficient enzymes. *bioRxiv* (2024). doi:10.1101/2024.05.03.592223
5. Madani, A., Krause, B., Greene, E. R., Subramanian, S., Mohr, B. P., Holton, J. M., Olmos, J. L., Jr, Xiong, C., Sun, Z. Z., Socher, R., Fraser, J. S. & Naik, N. Large language models generate functional protein sequences across diverse families. *Nat. Biotechnol.* **41**, 1099–1106 (2023).
6. Ertelt, M., Moretti, R., Meiler, J. & Schoeder, C. T. Self-supervised machine learning methods for protein design improve sampling but not the identification of high-fitness variants. *Sci. Adv.* **11**, eadr7338 (2025).
7. Kang, K., Setlur, A., Ghosh, D., Steinhardt, J., Tomlin, C., Levine, S. & Kumar, A. What do learning dynamics reveal about generalization in LLM reasoning? *arXiv [cs.LG]* (2024). at <<http://arxiv.org/abs/2411.07681>>
8. Dittert, S., Moens, V. & De Fabritiis, G. BricksRL: A platform for democratizing robotics and reinforcement learning research and education with LEGO. *arXiv [cs.RO]* (2024). at <<http://arxiv.org/abs/2406.17490>>
9. Mnih, V., Kavukcuoglu, K., Silver, D., Rusu, A. A., Veness, J., Bellemare, M. G., Graves, A., Riedmiller, M., Fidjeland, A. K., Ostrovski, G., Petersen, S., Beattie, C., Sadik, A., Antonoglou, I., King, H., Kumaran, D., Wierstra, D., Legg, S. & Hassabis, D. Human-level control through deep reinforcement learning. *Nature* **518**, 529–533 (2015).
10. Silver, D., Huang, A., Maddison, C. J., Guez, A., Sifre, L., van den Driessche, G., Schrittwieser, J., Antonoglou, I., Panneershelvam, V., Lanctot, M., Dieleman, S., Grewe, D., Nham, J., Kalchbrenner, N., Sutskever, I., Lillicrap, T., Leach, M., Kavukcuoglu, K., Graepel, T. & Hassabis, D. Mastering the game of Go with deep neural networks and tree search. *Nature* **529**, 484–489 (2016).
11. Silver, D., Hubert, T., Schrittwieser, J., Antonoglou, I., Lai, M., Guez, A., Lanctot, M., Sifre, L., Kumaran, D., Graepel, T., Lillicrap, T., Simonyan, K. & Hassabis, D. A general reinforcement learning algorithm that masters chess, shogi, and Go through self-play. *Science* **362**, 1140–1144 (2018).
12. Kiran, B. R., Sobh, I., Talpaert, V., Mannion, P., Sallab, A. A. A., Yogamani, S. & Pérez, P. Deep reinforcement learning for autonomous driving: A survey. *arXiv [cs.LG]* (2020). at <<http://arxiv.org/abs/2002.00444>>
13. Dayan, P. & Berridge, K. C. Model-based and model-free Pavlovian reward learning: revaluation, revision, and revelation. *Cogn. Affect. Behav. Neurosci.* **14**, 473–492 (2014).
14. Schulman, J., Wolski, F., Dhariwal, P., Radford, A. & Klimov, O. Proximal Policy Optimization Algorithms. *arXiv [cs.LG]* (2017). at <<http://arxiv.org/abs/1707.06347>>
15. Rafailov, R., Sharma, A., Mitchell, E., Ermon, S., Manning, C. D. & Finn, C. Direct Preference Optimization: Your language model is secretly a reward model. *arXiv [cs.LG]* (2023). at <<http://arxiv.org/abs/2305.18290>>
16. Shao, Z., Wang, P., Zhu, Q., Xu, R., Song, J., Zhang, M., Li, Y. K., Wu, Y. & Guo, D. DeepSeekMath: Pushing the limits of mathematical reasoning in open language models. *arXiv [cs.CL]* (2024). at <<http://arxiv.org/abs/2402.03300>>

17. DeepSeek-AI, Bi, X., Chen, D., Chen, G., Chen, S., Dai, D., Deng, C., Ding, H., Dong, K., Du, Q., Fu, Z., Gao, H., Gao, K., Gao, W., Ge, R., Guan, K., Guo, D., Guo, J., Hao, G., Hao, Z., He, Y., Hu, W., Huang, P., Li, E., Li, G., Li, J., Li, Y., Li, Y. K., Liang, W., Lin, F., Liu, A. X., Liu, B., Liu, W., Liu, X., Liu, X., Liu, Y., Lu, H., Lu, S., Luo, F., Ma, S., Nie, X., Pei, T., Piao, Y., Qiu, J., Qu, H., Ren, T., Ren, Z., Ruan, C., Sha, Z., Shao, Z., Song, J., Su, X., Sun, J., Sun, Y., Tang, M., Wang, B., Wang, P., Wang, S., Wang, Y., Wang, Y., Wu, T., Wu, Y., Xie, X., Xie, Z., Xie, Z., Xiong, Y., Xu, H., Xu, R. X., Xu, Y., Yang, D., You, Y., Yu, S., Yu, X., Zhang, B., Zhang, H., Zhang, L., Zhang, L., Zhang, M., Zhang, M., Zhang, W., Zhang, Y., Zhao, C., Zhao, Y., Zhou, S., Zhou, S., Zhu, Q. & Zou, Y. DeepSeek LLM: Scaling open-source language models with longtermism. *arXiv [cs.CL]* (2024). at <<http://arxiv.org/abs/2401.02954>>
18. ChatGPT. at <<https://chat.openai.com/chat>>
19. Gemini Team, Anil, R., Borgeaud, S., Wu, Y., Alayrac, J.-B., Yu, J., Soricut, R., Schalkwyk, J., Dai, A. M., Hauth, A., Millican, K., Silver, D., Petrov, S., Johnson, M., Antonoglou, I., Schrittwieser, J., Glaese, A., Chen, J., Pitler, E., Lillicrap, T., Lazaridou, A., Firat, O., Molloy, J., Isard, M., Barham, P. R., Hennigan, T., Lee, B., Viola, F., Reynolds, M., Xu, Y., Doherty, R., Collins, E., Meyer, C., Rutherford, E., Moreira, E., Ayoub, K., Goel, M., Tucker, G., Piqueras, E., Krikun, M., Barr, I., Savinov, N., Danihelka, I., Roelofs, B., White, A., Andreassen, A., von Glehn, T., Yagati, L., Kazemi, M., Gonzalez, L., Khalman, M., Sygnowski, J., Frechette, A., Smith, C., Culp, L., Proleev, L., Luan, Y., Chen, X., Lottes, J., Schucher, N., Lebron, F., Rrustemi, A., Clay, N., Crone, P., Kocisky, T., Zhao, J., Perz, B., Yu, D., Howard, H., Bloniarz, A., Rae, J. W., Lu, H., Sifre, L., Maggioni, M., Alcober, F., Garrette, D., Barnes, M., Thakoor, S., Austin, J., Barth-Maron, G., Wong, W., Joshi, R., Chaabouni, R., Fatiha, D., Ahuja, A., Liu, R., Li, Y., Cogan, S., Chen, J., Jia, C., Gu, C., Zhang, Q., Grimstad, J., Hartman, A. J., Chadwick, M., Tomar, G. S., Garcia, X., Senter, E., Taropa, E., Pillai, T. S., Devlin, J., Laskin, M., de Las Casas, D., Valter, D., Tao, C., Blanco, L., Badia, A. P., Reitter, D., Chen, M., Brennan, J., Rivera, C., Brin, S., Iqbal, S., Surita, G., Labanowski, J., Rao, A., Winkler, S., Parisotto, E., Gu, Y., Olszewska, K., Zhang, Y., Addanki, R., Miech, A., Louis, A., El Shafey, L., Teplyashin, D., Brown, G., Catt, E., Attaluri, N., Balaguer, J., Xiang, J., Wang, P., Ashwood, Z., Briukhov, A., Webson, A., Ganapathy, S., Sanghavi, S., Kannan, A., Chang, M.-W., Stjerngren, A., Djolonga, J., Sun, Y., Bapna, A., Aitchison, M., Pejman, P., Michalewski, H., Yu, T., Wang, C., Love, J., Ahn, J., Bloxwich, D., Han, K., Humphreys, P., Sellam, T., Bradbury, J., Godbole, V., Samangooei, S., Damoc, B., Kaskasoli, A., Arnold, S. M. R., Vasudevan, V., Agrawal, S., Riesa, J., Lepikhin, D., Tanburn, R., Srinivasan, S., Lim, H., Hodkinson, S., Shyam, P., Ferret, J., Hand, S., Garg, A., Le Paine, T., Li, J., Li, Y., Giang, M., Neitz, A., Abbas, Z., York, S., Reid, M., Cole, E., Chowdhery, A., Das, D., Rogozińska, D., Nikolaev, V., Sprechmann, P., Nado, Z., Zilka, L., Prost, F., He, L., Monteiro, M., Mishra, G., Welty, C., Newlan, J., Jia, D., Allamanis, M., Hu, C. H., de Liedekerke, R., Gilmer, J., Saroufim, C., Rijhwani, S., Hou, S., Shrivastava, D., Baddepudi, A., Goldin, A., Ozturel, A., Cassirer, A., Xu, Y., Sohn, D., Sachan, D., Amplayo, R. K., Swanson, C., Petrova, D., Narayan, S., Guez, A., Brahma, S., Landon, J., Patel, M., Zhao, R., Villela, K., Wang, L., Jia, W., Rahtz, M., Giménez, M., Yeung, L., Lin, H., Keeling, J., Georgiev, P., Mincu, D., Wu, B., Haykal, S., Saputro, R., Vodrahalli, K., Qin, J., Cankara, Z., Sharma, A., Fernando, N., Hawkins, W., Neyshabur, B., Kim, S., Hutter, A., Agrawal, P., Castro-Ros, A., van den Driessche, G., Wang, T., Yang, F., Chang, S.-Y., Komarek, P., McIlroy, R., Lučić, M., Zhang, G., Farhan, W., Sharman, M., Natsev, P., Michel, P., Cheng, Y., Bansal, Y., Qiao, S., Cao, K., Shakeri, S., Butterfield, C., Chung, J., Rubenstein, P. K., Agrawal, S., Mensch, A., Soparkar, K., Lenc, K., Chung, T., Pope, A., Maggiore, L., Kay, J., Jhakra, P., Wang, S., Maynez, J., Phuong, M., Tobin, T., Tacchetti, A., Trebacz, M., Robinson, K., Katariya, Y., Riedel, S., Bailey, P., Xiao, K., Ghelani, N., Aroyo, L., Slone, A., Houlshby, N., Xiong, X., Yang, Z., Gribovskaya, E., Adler, J., Wirth, M., Lee, L., Music Li, Kagohara, T., Pavagadhi, J., Bridgers, S., Bortsova, A., Ghemawat, S., Ahmed, Z., Liu, T., Powell, R., Bolina, V., Iinuma, M., Zablotskaia, P., Besley, J., Chung, D.-W.,

Dozat, T., Comanescu, R., Si, X., Greer, J., Su, G., Polacek, M., Kaufman, R. L., Tokumine, S., Hu, H., Buchatskaya, E., Miao, Y., Elhawaty, M., Siddhant, A., Tomasev, N., Xing, J., Greer, C., Miller, H., Ashraf, S., Roy, A., Zhang, Z., Ma, A., Filos, A., Besta, M., Blevins, R., Klimenko, T., Yeh, C.-K., Changpinyo, S., Mu, J., Chang, O., Pajarskas, M., Muir, C., Cohen, V., Le Lan, C., Haridasan, K., Marathe, A., Hansen, S., Douglas, S., Samuel, R., Wang, M., Austin, S., Lan, C., Jiang, J., Chiu, J., Lorenzo, J. A., Sjöstrand, L. L., Cevey, S., Gleicher, Z., Avrahami, T., Boral, A., Srinivasan, H., Selo, V., May, R., Aisopos, K., Hussenot, L., Soares, L. B., Baumli, K., Chang, M. B., Recasens, A., Caine, B., Pritzel, A., Pavetic, F., Pardo, F., Gergely, A., Frye, J., Ramasesh, V., Horgan, D., Badola, K., Kassner, N., Roy, S., Dyer, E., Campos, V., Tomala, A., Tang, Y., El Badawy, D., White, E., Mustafa, B., Lang, O., Jindal, A., Vikram, S., Gong, Z., Caelles, S., Hemsley, R., Thornton, G., Feng, F., Stokowiec, W., Zheng, C., Thacker, P., Ünlü, Ç., Zhang, Z., Saleh, M., Svensson, J., Bileschi, M., Patil, P., Anand, A., Ring, R., Tsihlias, K., Vezer, A., Selvi, M., Shevlane, T., Rodriguez, M., Kwiatkowski, T., Daruki, S., Rong, K., Dafoe, A., FitzGerald, N., Gu-Lemberg, K., Khan, M., Hendricks, L. A., Pellat, M., Feinberg, V., Cobon-Kerr, J., Sainath, T., Rauh, M., Hashemi, S. H., Ives, R., Hasson, Y., Li, Y., Noland, E., Cao, Y., Byrd, N., Hou, L., Wang, Q., Sottiaux, T., Paganini, M., Lespiau, J.-B., Moufarek, A., Hassan, S., Shivakumar, K., van Amersfoort, J., Mandhane, A., Joshi, P., Goyal, A., Tung, M., Brock, A., Sheahan, H., Misra, V., Li, C., Rakićević, N., Dehghani, M., Liu, F., Mittal, S., Oh, J., Noury, S., Sezener, E., Huot, F., Lamm, M., De Cao, N., Chen, C., Elsayed, G., Chi, E., Mahdieh, M., Tenney, I., Hua, N., Petrychenko, I., Kane, P., Scandinaro, D., Jain, R., Uesato, J., Datta, R., Sadovsky, A., Bunyan, O., Rabiej, D., Wu, S., Zhang, J., Vasudevan, G., Leurent, E., Alnahlawi, M., Georgescu, I., Wei, N., Zheng, I., Chan, B., Rabinovitch, P. G., Stanczyk, P., Zhang, Y., Steiner, D., Naskar, S., Azzam, M., Johnson, M., Paszke, A., Chiu, C.-C., Elias, J. S., Mohiuddin, A., Muhammad, F., Miao, J., Lee, A., Vieillard, N., Potluri, S., Park, J., Davoodi, E., Zhang, J., Stanway, J., Garmon, D., Karmarkar, A., Dong, Z., Lee, J., Kumar, A., Zhou, L., Evens, J., Isaac, W., Chen, Z., Jia, J., Levskaya, A., Zhu, Z., Gorgolewski, C., Grabowski, P., Mao, Y., Magni, A., Yao, K., Snaider, J., Casagrande, N., Suganthan, P., Palmer, E., Irving, G., Loper, E., Faruqui, M., Arkatkar, I., Chen, N., Shafran, I., Fink, M., Castaño, A., Giannoumis, I., Kim, W., Rybiński, M., Sreevatsa, A., Prendki, J., Soergel, D., Goedeckemeyer, A., Gierke, W., Jafari, M., Gaba, M., Wiesner, J., Wright, D. G., Wei, Y., Vashisht, H., Kulizhskaya, Y., Hoover, J., Le, M., Li, L., Iwuanyanwu, C., Liu, L., Ramirez, K., Khorlin, A., Cui, A., Tian, L. I. N., Georgiev, M., Wu, M., Aguilar, R., Pallo, K., Chakladar, A., Repina, A., Wu, X., van der Weide, T., Ponnappalli, P., Kaplan, C., Simsa, J., Li, S., Dousse, O., Yang, F., Piper, J., Ie, N., Lui, M., Pasumarthi, R., Lintz, N., Vijayakumar, A., Thiet, L. N., Andor, D., Valenzuela, P., Paduraru, C., Peng, D., Lee, K., Zhang, S., Greene, S., Nguyen, D. D., Kurylowicz, P., Velury, S., Krause, S., Hardin, C., Dixon, L., Janzer, L., Choo, K., Feng, Z., Zhang, B., Singhal, A., Latkar, T., Zhang, M., Le, Q., Abellan, E. A., Du, D., McKinnon, D., Antropova, N., Bolukbasi, T., Keller, O., Reid, D., Finchelstein, D., Raad, M. A., Crocker, R., Hawkins, P., Dadashi, R., Gaffney, C., Lall, S., Franko, K., Filonov, E., Bulanova, A., Leblond, R., Yadav, V., Chung, S., Askham, H., Cobo, L. C., Xu, K., Fischer, F., Xu, J., Sorokin, C., Alberti, C., Lin, C.-C., Evans, C., Zhou, H., Dimitriev, A., Forbes, H., Banarse, D., Tung, Z., Liu, J., Omernick, M., Bishop, C., Kumar, C., Sterneck, R., Foley, R., Jain, R., Mishra, S., Xia, J., Bos, T., Cideron, G., Amid, E., Piccinno, F., Wang, X., Banzal, P., Gurita, P., Noga, H., Shah, P., Mankowitz, D. J., Polozov, A., Kushman, N., Krakovna, V., Brown, S., Bateni, M., Duan, D., Firoiu, V., Thotakuri, M., Natan, T., Mohananey, A., Geist, M., Mudgal, S., Girgin, S., Li, H., Ye, J., Roval, O., Tojo, R., Kwong, M., Lee-Thorp, J., Yew, C., Yuan, Q., Bagri, S., Sinopalnikov, D., Ramos, S., Mellor, J., Sharma, A., Severyn, A., Lai, J., Wu, K., Cheng, H.-T., Miller, D., Sonnerat, N., Vnukov, D., Greig, R., Beattie, J., Caveness, E., Bai, L., Eisenschlos, J., Korchemniy, A., Tsai, T., Jasarevic, M., Kong, W., Dao, P., Zheng, Z., Liu, F., Yang, F., Zhu, R., Geller, M., Teh, T. H., Sanmiya, J., Gladchenko, E., Trdin, N., Sozanschi, A., Toyama, D., Rosen, E., Tavakkol, S., Xue, L., Elkind, C., Woodman, O., Carpenter, J.,

- Papamakarios, G., Kemp, R., Kafle, S., Grunina, T., Sinha, R., Talbert, A., Goyal, A., Wu, D., Owusu-Afriyie, D., Du, C., Thornton, C., Pont-Tuset, J., Narayana, P., Li, J., Fatehi, S., Wieting, J., Ajmeri, O., Uria, B., Zhu, T., Ko, Y., Knight, L., Héliou, A., Niu, N., Gu, S., Pang, C., Tran, D., Li, Y., Levine, N., Stolovich, A., Kalb, N., Santamaria-Fernandez, R., Goenka, S., Yustalim, W., Strudel, R., Elqursh, A., Lakshminarayanan, B., Deck, C., Upadhyay, S., Lee, H., Dusenberry, M., Li, Z., Wang, X., Levin, K., Hoffmann, R., Holtmann-Rice, D., Bachem, O., Yue, S., Arora, S., Malmi, E., Mirylenka, D., Tan, Q., Koh, C., Yeganeh, S. H., Pöder, S., Zheng, S., Pongetti, F., Tariq, M., Sun, Y., Ionita, L., Seyedhosseini, M., Tafti, P., Kotikalapudi, R., Liu, Z., Gulati, A., Liu, J., Ye, X., Chrzaszcz, B., Wang, L., Sethi, N., Li, T., Brown, B., Singh, S., Fan, W., Parisi, A., Stanton, J., Kuang, C., Koverkathu, V., Choquette-Choo, C. A., Li, Y., Lu, T. J., Ittycheriah, A., Shroff, P., Sun, P., Varadarajan, M., Bahargam, S., Willoughby, R., Gaddy, D., Dasgupta, I., Desjardins, G., Cornero, M., Robenek, B., Mittal, B., Albrecht, B., Shenoy, A., Moiseev, F., Jacobsson, H., Ghaffarkhah, A., Rivière, M., Walton, A., Crepy, C., Parrish, A., Liu, Y., Zhou, Z., Farabet, C., Radebaugh, C., Srinivasan, P., van der Salm, C., Fidjeland, A., Scellato, S., Latorre-Chimoto, E., Klimczak-Plucińska, H., Bridson, D., de Cesare, D., Hudson, T., Mendolicchio, P., Walker, L., Morris, A., Penchev, I., Mauger, M., Guseynov, A., Reid, A., Odoom, S., Loher, L., Cotruta, V., Yenugula, M., Grewe, D., Petrushkina, A., Duerig, T., Sanchez, A., Yadlowsky, S., Shen, A., Globerson, A., Kurzrok, A., Webb, L., Dua, S., Li, D., Lahoti, P., Bhupatiraju, S., Hurt, D., Qureshi, H., Agarwal, A., Shani, T., Eyal, M., Khare, A., Belle, S. R., Wang, L., Tekur, C., Kale, M. S., Wei, J., Sang, R., Saeta, B., Liechty, T., Sun, Y., Zhao, Y., Lee, S., Nayak, P., Fritz, D., Vuyyuru, M. R., Aslanides, J., Vyas, N., Wicke, M., Ma, X., Bilal, T., Eltyshv, E., Balle, D., Martin, N., Cate, H., Manyika, J., Amiri, K., Kim, Y., Xiong, X., Kang, K., Luisier, F., Tripuraneni, N., Madras, D., Guo, M., Waters, A., Wang, O., Ainslie, J., Baldridge, J., Zhang, H., Pruthi, G., Bauer, J., Yang, F., Mansour, R., Gelman, J., Xu, Y., Polovets, G., Liu, J., Cai, H., Chen, W., Sheng, X., Xue, E., Ozair, S., Yu, A., Angermueller, C., Li, X., Wang, W., Wiesinger, J., Koukoumidis, E., Tian, Y., Iyer, A., Gurumurthy, M., Goldenson, M., Shah, P., Blake, M. K., Yu, H., Urbanowicz, A., Palomaki, J., Fernando, C., Brooks, K., Durden, K., Mehta, H., Momchev, N., Rahimtoroghi, E., Georgaki, M., Raul, A., Ruder, S., Redshaw, M., Lee, J., Jalan, K., Li, D., Perng, G., Hechtman, B., Schuh, P., Nasr, M., Chen, M., Milan, K., Mikulik, V., Strohmaier, T., Franco, J., Green, T., Hassabis, D., Kavukcuoglu, K., Dean, J. & Vinyals, O. Gemini: A Family of Highly Capable Multimodal Models. *arXiv [cs.CL]* (2023). at <<http://arxiv.org/abs/2312.11805>>
20. Angermueller, C. & Dohan, D. Model-based reinforcement learning for biological sequence design. at <<https://storage.googleapis.com/gweb-research2023-media/pubtools/5917.pdf>>
 21. Widatalla, T., Rafailov, R. & Hie, B. Aligning protein generative models with experimental fitness via Direct Preference Optimization. *bioRxiv* (2024). doi:10.1101/2024.05.20.595026
 22. Mistani, P. & Mysore, V. Preference optimization of protein language models as a multi-objective binder design paradigm. *arXiv [physics.bio-ph]* (2024). at <<http://arxiv.org/abs/2403.04187>>
 23. Bhatnagar, A., Jain, S., Beazer, J., Curran, S. C., Hoffnagle, A. M., Ching, K., Martyn, M., Nayfach, S., Ruffolo, J. A. & Madani, A. Scaling unlocks broader generation and deeper functional understanding of proteins. *bioRxiv* 2025.04.15.649055 (2025). doi:10.1101/2025.04.15.649055
 24. Blalock, N., Seshadri, S., Babbar, A., Fahlberg, S. A., Kulkarni, A. & Romero, P. A. Functional alignment of protein language models via reinforcement learning. *bioRxiv* 2025.05.02.651993 (2025). doi:10.1101/2025.05.02.651993
 25. Kenton, Z., Everitt, T., Weidinger, L., Gabriel, I., Mikulik, V. & Irving, G. Alignment of language agents. *arXiv [cs.AI]* (2021). at <<http://arxiv.org/abs/2103.14659>>
 26. Yu, T., Cui, H., Li, J. C., Luo, Y., Jiang, G. & Zhao, H. Enzyme function prediction using contrastive learning. *Science* **379**, 1358–1363 (2023).

27. Meier, J., Rao, R., Verkuil, R., Liu, J., Sercu, T. & Rives, A. Language models enable zero-shot prediction of the effects of mutations on protein function. *Synthetic Biology* (2021). at <<https://www.biorxiv.org/content/10.1101/2021.07.09.450648v1.full>>
28. Dauparas, J., Anishchenko, I., Bennett, N., Bai, H., Ragotte, R. J., Milles, L. F., Wicky, B. I. M., Courbet, A., de Haas, R. J., Bethel, N., Leung, P. J. Y., Huddy, T. F., Pellock, S., Tischer, D., Chan, F., Koepnick, B., Nguyen, H., Kang, A., Sankaran, B., Bera, A. K., King, N. P. & Baker, D. Robust deep learning-based protein sequence design using ProteinMPNN. *Science* **378**, 49–56 (2022).
29. Johnson, S. R., Fu, X., Viknander, S., Goldin, C., Monaco, S., Zelezniak, A. & Yang, K. K. Computational Scoring and Experimental Evaluation of Enzymes Generated by Neural Networks. *bioRxiv* 2023.03.04.531015 (2023). doi:10.1101/2023.03.04.531015
30. Armer, C., Kane, H., Cortade, D. L., Redestig, H., Estell, D. A., Yusuf, A., Rollins, N., Spinner, H., Marks, D., Brunette, T. J., Kelly, P. J. & DeBenedictis, E. Results of the Protein Engineering Tournament: An open science benchmark for protein modeling and design. *bioRxiv* (2024). doi:10.1101/2024.08.12.606135
31. Rafailov, R., Hejna, J., Park, R. & Finn, C. From r to Q^{*}: Your Language Model is Secretly a Q-Function. *arXiv [cs.LG]* (2024). at <<http://arxiv.org/abs/2404.12358>>
32. van Kempen, M., Kim, S. S., Tumescheit, C., Mirdita, M., Lee, J., Gilchrist, C. L. M., Söding, J. & Steinegger, M. Fast and accurate protein structure search with Foldseek. *Nat. Biotechnol.* **42**, 243–246 (2024).
33. Rives, A., Meier, J., Sercu, T., Goyal, S., Lin, Z., Liu, J., Guo, D., Ott, M., Zitnick, C. L., Ma, J. & Fergus, R. Biological structure and function emerge from scaling unsupervised learning to 250 million protein sequences. *Proc. Natl. Acad. Sci. U. S. A.* **118**, e2016239118 (2021).
34. Schmirler, R., Heinzinger, M. & Rost, B. Fine-tuning protein language models boosts predictions across diverse tasks. *Nat. Commun.* **15**, 7407 (2024).
35. Cotet, T.-S., Krawczuk, I., Stocco, F., Ferruz, N., Gitter, A., Kurumida, Y., de Almeida Machado, L., Paesani, F., Calia, C. N., Challacombe, C. A., Haas, N., Qamar, A., Correia, B. E., Pacesa, M., Nickel, L., Subr, K., Castorina, L. V., Campbell, M. J., Ferragu, C., Kidger, P., Hallee, L., Wood, C. W., Stam, M. J., Kluonis, T., Ünal, S. M., Belot, E., Naka, A. & Organizers, A. C. Crowdsourced protein design: Lessons from the Adapticv EGFR binder competition. *bioRxiv* (2025). doi:10.1101/2025.04.17.648362

Supplementary Information for:

Guiding Protein Language Models with Reinforcement Learning

Filippo Stocco^{1,2}, Maria Artigues-Lleixà^{1,2}, Andrea Hunklinger^{2,3}, Talal Widatalla^{4,5},
Marc Güell^{1,6}, Noelia Ferruz^{2,1,*}

¹Department of Medicine and Life Sciences, Universitat Pompeu Fabra, Barcelona, Spain

²Centre for Genomic Regulation, the Barcelona Institute of Science and Technology, Dr Aiguader 88, Barcelona 08003, Spain

³Universitat de Barcelona, Facultat de Farmàcia i Ciències de l'Alimentació, Avda. Diagonal 643, Barcelona 08028, Spain

⁴Stanford University,

⁵Arc Institute

⁶ICREA, Institució Catalana de Recerca i Estudis Avançats, Barcelona, Spain

*E-mail: noelia.ferruz@crg.eu

Table of Contents:

Figures S1 – S10

Tables S1 – S3

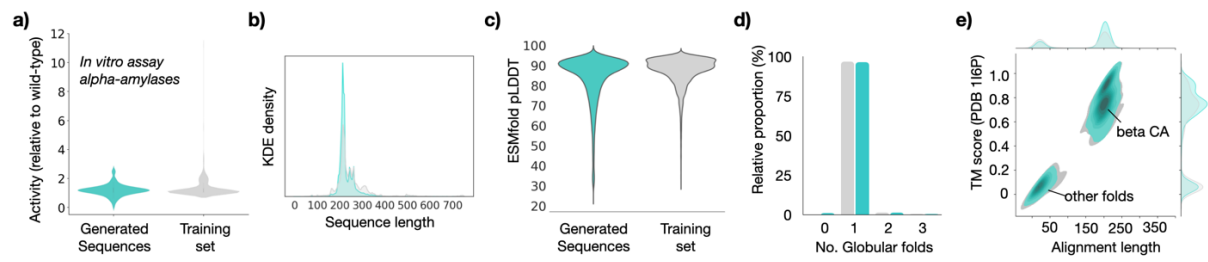


Figure S1: pLMs mirror the distributions of their underlying training sets for multiple properties. This behaviour occurs across different properties, including experimental data on the activity of generated and natural alpha amylases (a), lengths (b), predicted pLDDT values (c), number of domains (d), or topologies (e).

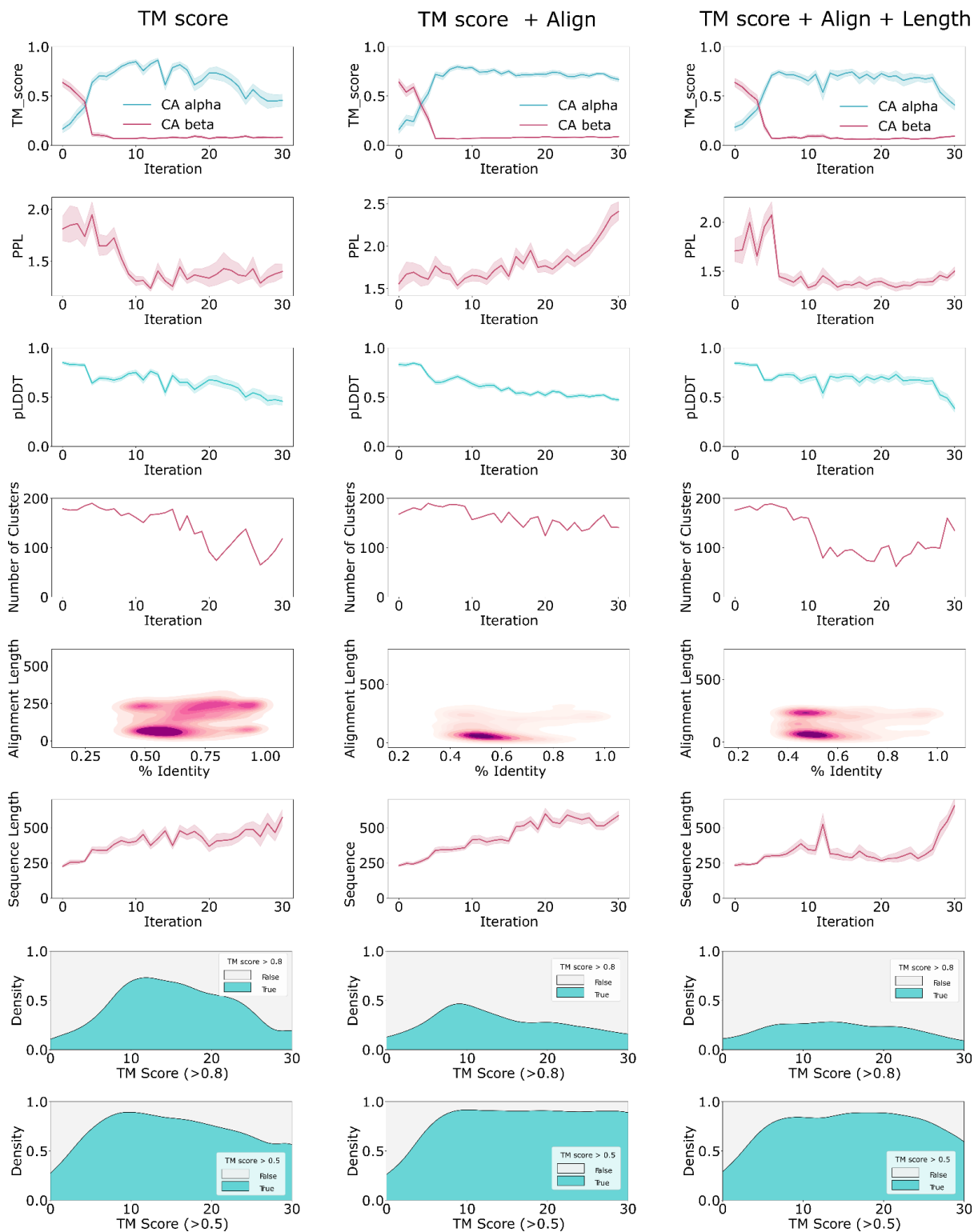


Figure S2: DPO-guided topology generation using TM-score as an oracle. We evaluated the framework at increasing the proportion of generated alpha carbonic anhydrases (CA) per iteration, using TM-score as the reward function alone (left), TM-score and alignment length as a composite function (central), and TM-score, a Gaussian equation of length and alignment length (right). We record several properties, namely, in row order: TM-score against alpha CA pdb 2VVB, perplexity (PPL) of the model, ESMFold pLDDT, number of clusters at 80% as computed with MMseqs2, similarity to the training set, sequence length, density of proteins showing TM-scores over 0.8, and over 0.5.

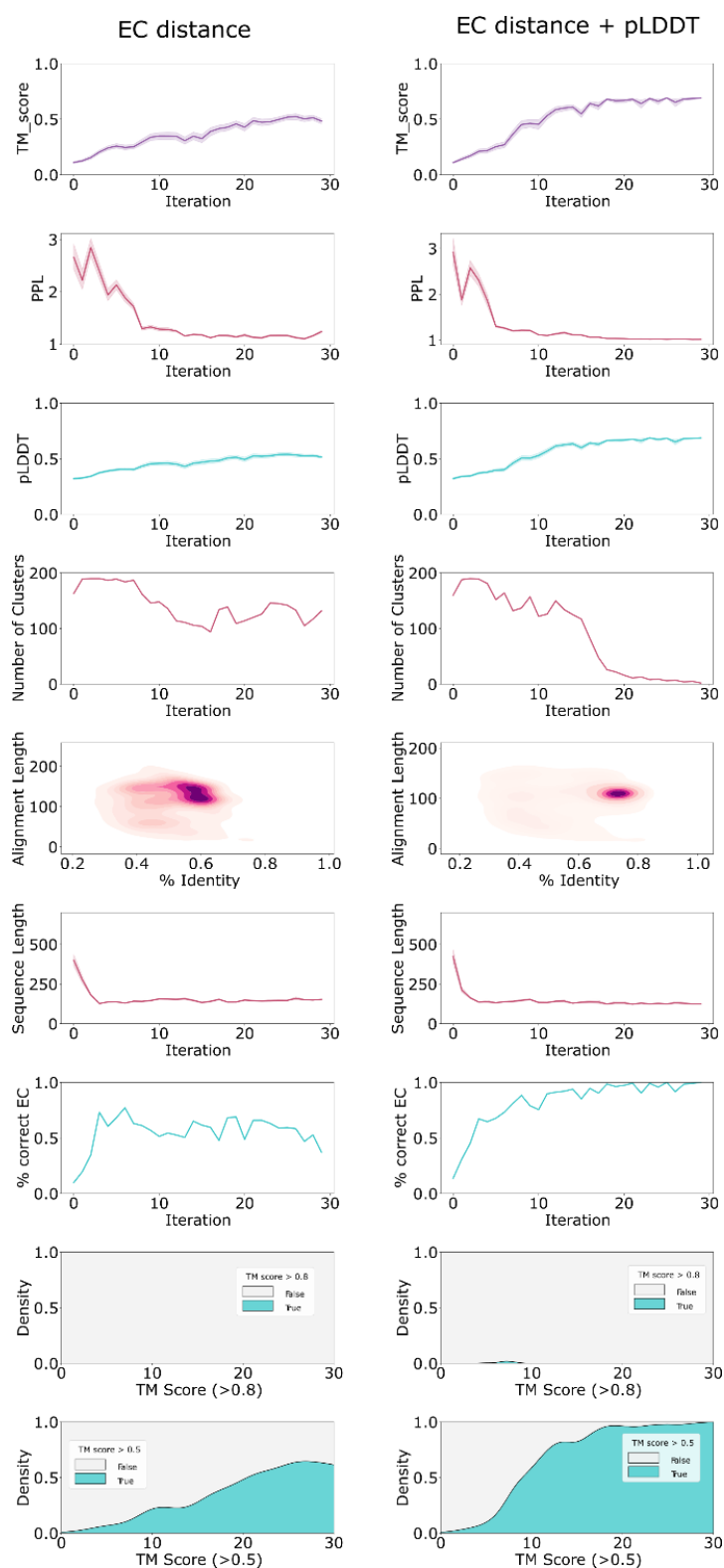


Figure S3: DPO implementations for the optimization of CLEAN-labelled sequences, considering CLEAN embeddings only or with pLDDT values as part of the scoring as well.

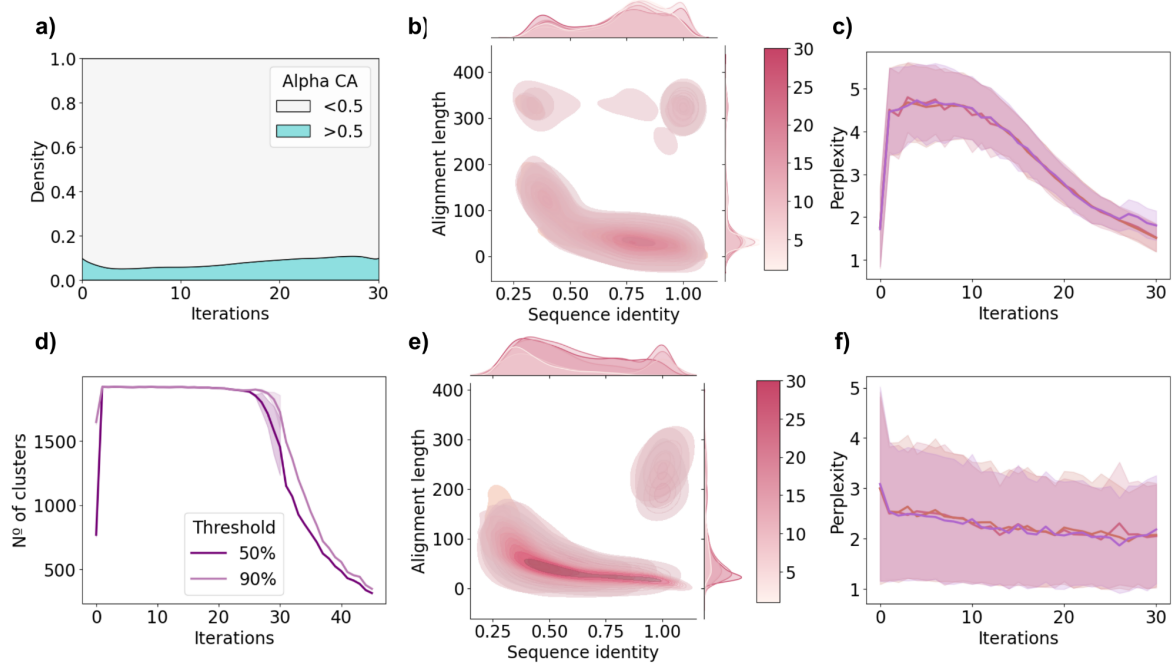


Figure S4: self-FT-guided topology and enzyme functional annotation generation. (a) Proportion of generated sequences with more or less than 0.5 TM-score when superimposed with PDB 2VVB with TM-score as a reward function. (b) Distribution of sequence similarity of synthetic sequences generated against the 200 sequences set used to finetune the model the previous iteration for the TM-score reward function. (c) Perplexity of the generated sequences with the TM-score reward function across 30 iterations. (d) Progression of the number of clusters of sequences with TM-score reward function until 45 iterations. (e) Distribution of sequence similarity of synthetic sequences generated against the 200 sequences set used to finetune the model the previous iteration got the CLEAN reward function. (f) Perplexity of the generated sequences with the CLEAN reward function across 30 iterations.

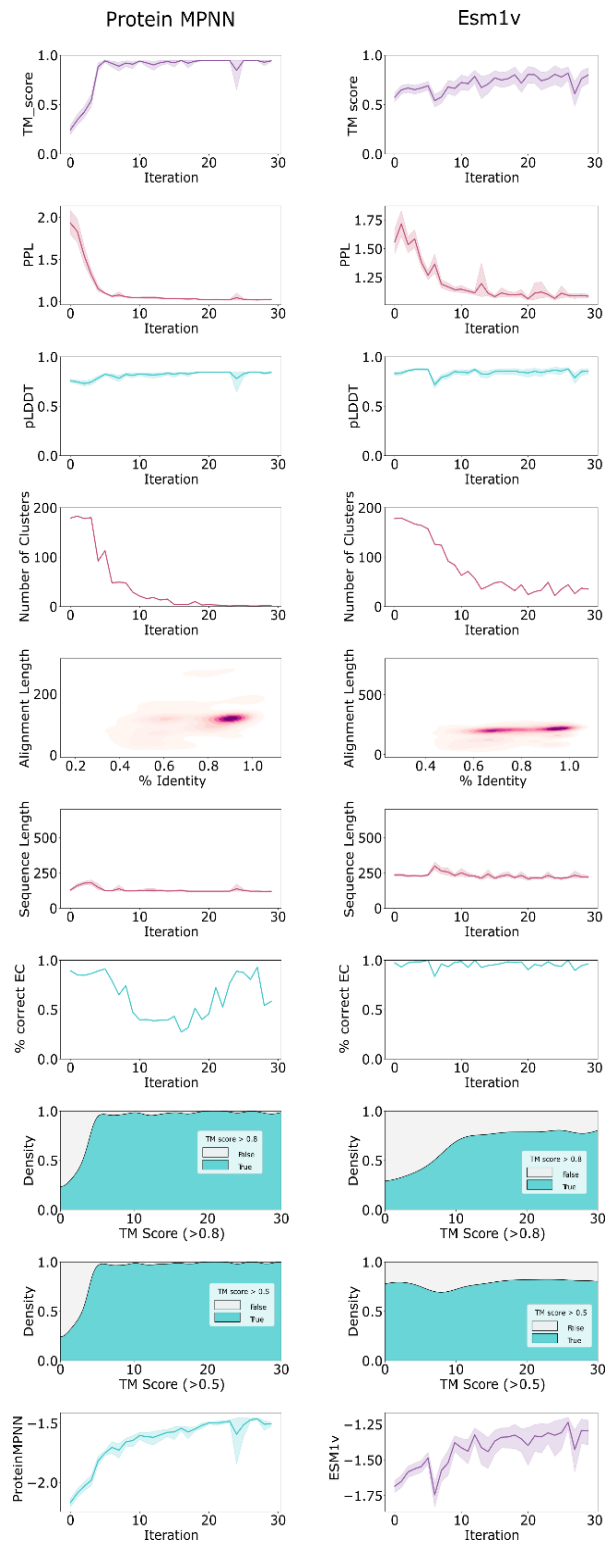


Figure S5: DPO-guided numerical generation using ESM-1v and ProteinMPNN as an oracle. We evaluated the framework at increasing both statistical scores per iteration, using ESM-1v (right) and ProteinMPNN (left) as the reward function alone. We record several properties, namely, in row order: TM-score against α CA PDB 2VVB, perplexity (PPL) of the model, ESMFold pLDDT, number of clusters at 80% as computed with MMseqs2, similarity to the training set, sequence length, density of proteins showing TM-scores over 0.8 and over 0.5 and ESM-1v and ProteinMPNN scores.

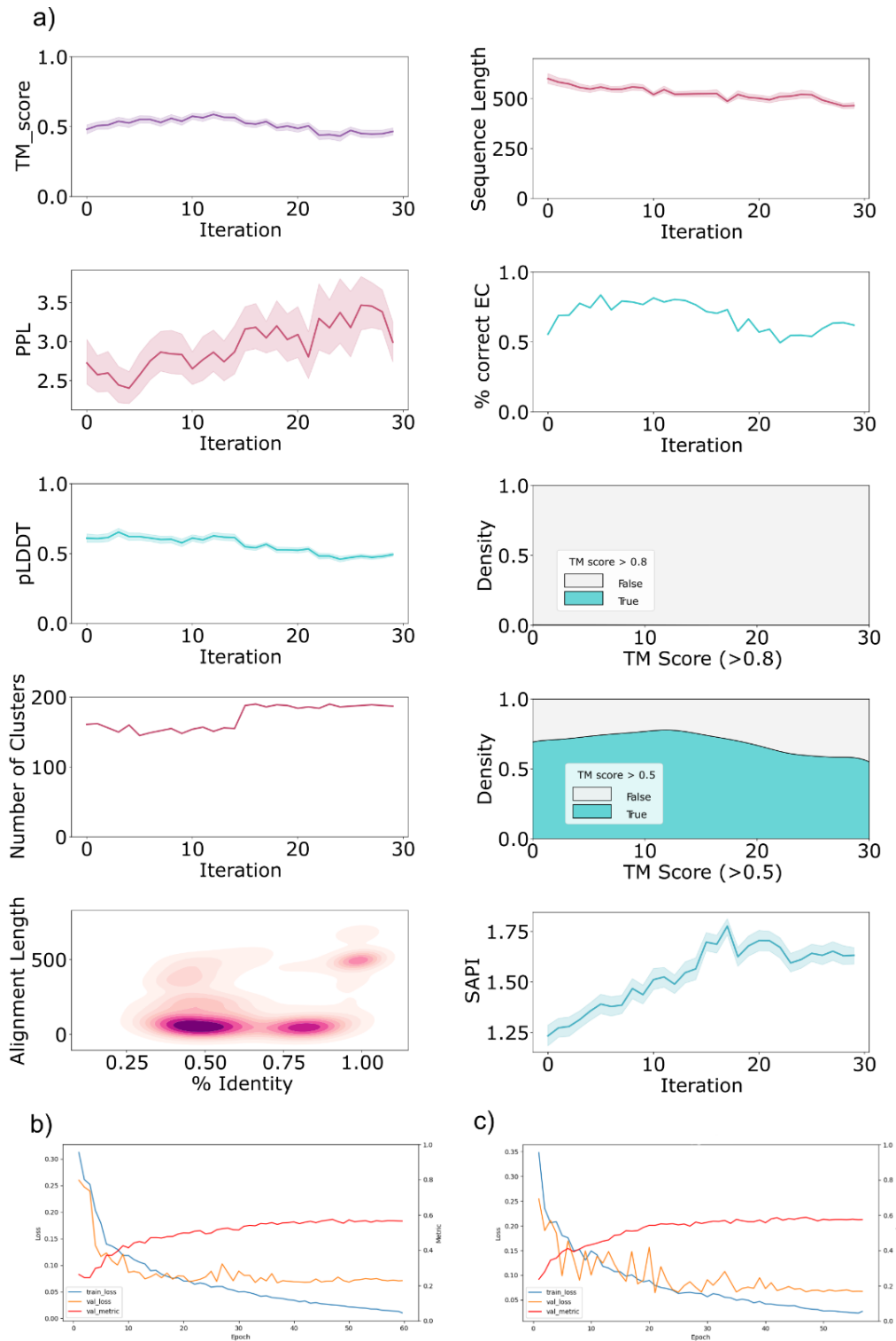


Figure S6: DPO Optimized for Activity Prediction **a)** Progression of key metrics during the reinforcement campaign, highlighting the maximization of activity as the objective. No substantial decline is observed in metrics such as TM score, perplexity (ppl), or pLDDT. **(b), (c)** Training curves for regression models predicting activity from input sequences. Models were constructed using ESM2 or ESM1v architectures and fine-tuned with LoRA for a single-label output. In both cases, the Spearman correlation coefficient (red line) achieved a value of 0.6.

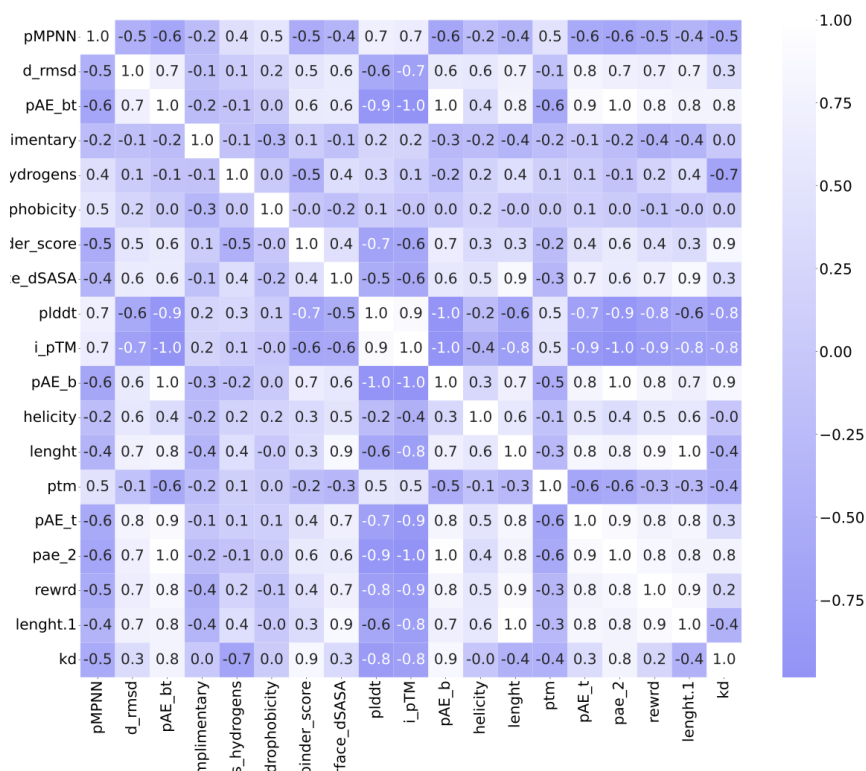
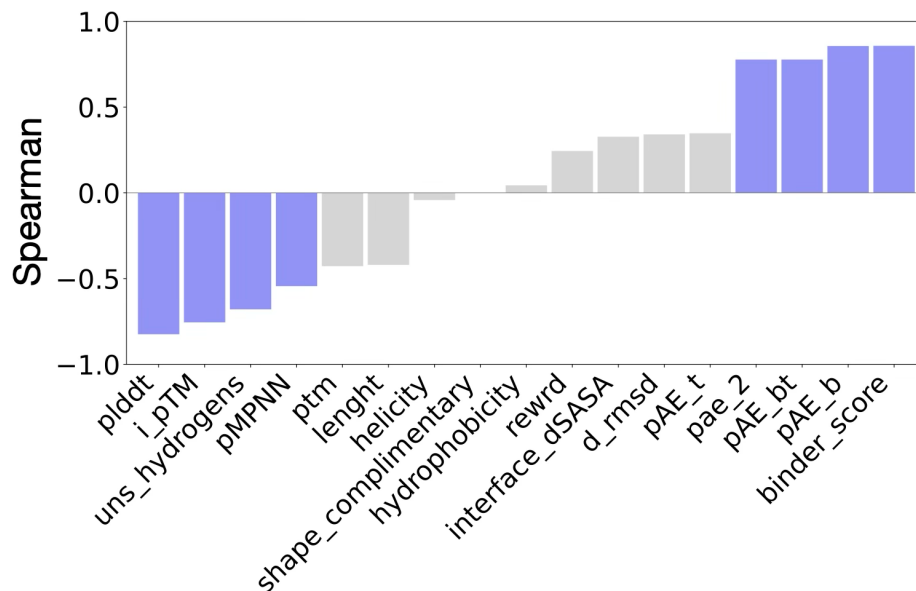


Figure S7: Spearman correlation of the in silico metrics with experimental values from round 2. The right panel shows the correlation matrix with experimental data (K_D) against some in silico metrics, while the left panel provides a close-up of the correlation between K_D and the metrics. The columns in purple on the left have a correlation higher than 0.5 or lower than -0.5.

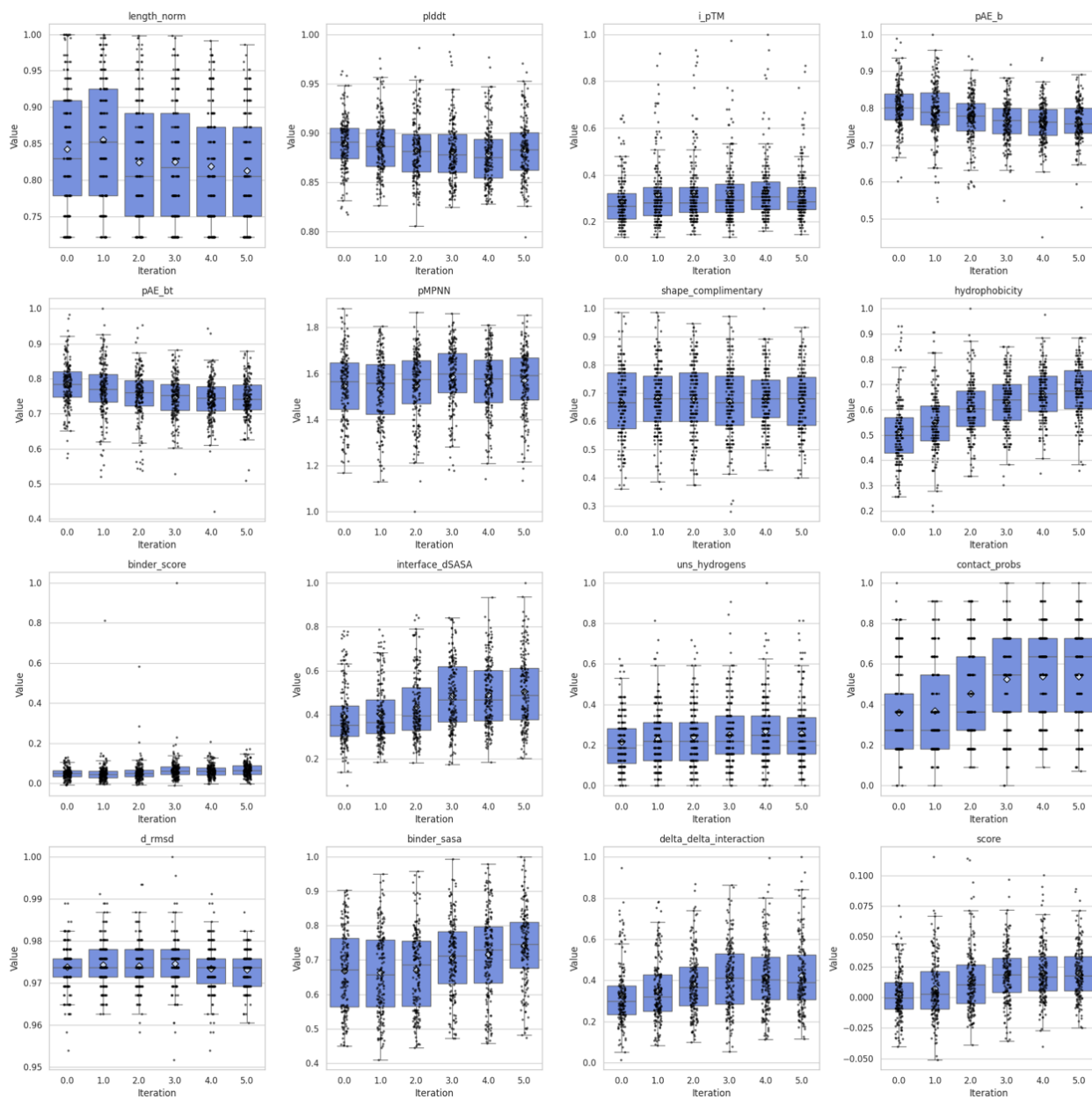


Figure S8: In silico metrics can be used to compose a multiobjective scoring function to be maximise. Here as an example, a reinforcement campaign with in-silico metrics that showed correlated with the experimental data of round 1 and in previous studies [ref] (see Figure S9) to bind CD80. The score is the weighted average based on the correlation matrix in Figure S9. Max() normalization is applied on each metric before summing.

```

kllQuery_11813779 S N T V Q R C P S S H D A Y C L Y G G V C F Y I P E M E S F A C K C V K G F V G R C Q F S D L E W W E
ref|XP_028445999.1|:888-939 S N S I E S C P S S H D S Y C L Y G G V C F Y F P E M E S Y A C N C V A G Y V G R C Q F S D L E W W E
gb|KAI8015452.1|:319-369 - N A V E S C P S S H D T Y C F Y G G V C F Y L P E M E S Y A C N C I A G Y I G R C Q F S D L E W W E
ref|XP_053179658.1|:887-938 S N S V Q S C P S S H E S Y C L Y E G I C F Y F P E M E S Y A C N C V S G Y M G R C Q F S D L E W W E
ref|XP_039670365.1|:946-997 S N S I E S C P S T H D S Y C L Y G G V C F Y F P E M E S Y A C N C V A G Y V G R C Q F S D L E W W E
ref|XP_035856948.1|:946-997 S N S I E S C P S T H D S Y C L Y G G V C F Y F P E M E S Y A C N C V A G Y V G R C Q F S D L E W W E
ref|XP_051505623.1|:992-1042 - N T V Q S C P S T H D S Y C L Y E G V C L Y F P E M E S Y A C K C V P G Y M G R C Q F S D L E W W E
ref|XP_023849523.1|:989-1040 T N T V E S C P S S H D T Y C L Y E G V C F Y F P E M E S Y A C N C I S G Y M G R C Q F S D L E W W E
ref|XP_014067428.1|:955-1006 T N T V E S C P S S H D T Y C L Y E G V C F Y F P E M E S Y A C N C I S G Y M G R C Q F S D L E W W E
emb|CAI1059042.1|:936-987 S N S V E S C P S T H D S Y C L Y G G V C F Y F P E M E S Y A C N C V S G Y M G R C Q F S D L E W W E
ref|XP_029626642.1|:994-1045 T N T V E S C P S S H D T Y C L Y E G V C F Y F P E M E S Y A C N C I S G Y M G R C Q F S D L E W W E
ref|XP_014067426.1|:985-1036 T N T V E S C P S S H D T Y C L Y E G V C F Y F P E M E S Y A C N C I S G Y M G R C Q F S D L E W W E
ref|XP_014067427.1|:983-1034 T N T V E S C P S S H D T Y C L Y E G V C F Y F P E M E S Y A C N C I S G Y M G R C Q F S D L E W W E
ref|XP_021439780.2|:985-1036 T N T V E S C P S S H D T Y C L Y E G V C F Y F P E M E S Y A C N C I S G Y M G R C Q F S D L E W W E
gb|KAI7801842.1|:886-937 N N S V Q S C P S T H D S Y C L Y E G V C F Y F P E M E S Y A C N C V S G Y L G R C Q F S D L E W W E
ref|XP_071266682.1|:983-1034 T N T V E S C P S S H D T Y C L Y E G V C F Y F P E M E S Y A C N C I S G Y M G R C Q F S D L E W W E
ref|XP_071266681.1|:985-1036 T N T V E S C P S S H D T Y C L Y E G V C F Y F P E M E S Y A C N C I S G Y M G R C Q F S D L E W W E
ref|XP_038867583.1|:907-958 T N T V E S C P S S H D T Y C L Y E G V C F Y F P E M E S Y A C N C I S G Y M G R C Q F S D L E W W E
ref|XP_055745254.1|:985-1036 T N T V E S C P S S H D T Y C L Y E G V C F Y F P E M E S Y A C N C I S G Y M G R C Q F S D L E W W E
ref|XP_064874306.1|:990-1041 T N T V E S C P S S H D T Y C L Y E G V C F Y F P E M E S Y A C N C I S G Y M G R C Q F S D L E W W E
ref|XP_064874306.1|:985-1036 T N T V E S C P S S H D T Y C L Y E G V C F Y F P E M E S Y A C N C I S G Y M G R C Q F S D L E W W E
ref|XP_070994528.1|:985-1036 T N T V E S C P S S H D T Y C L Y E G V C F Y F P E M E S Y A C N C I S G Y M G R C Q F S D L E W W E
ref|XP_026186736.1|:948-999 S N S V Q S C P S T H E S Y C L Y G G V C F Y F P E M E S Y A C N C V S G Y M G R C Q F S D L E W W E
ref|XP_057205121.1|:928-979 N N S V Q S C P S T H D S Y C L Y E G V C F Y F P E M E S Y A C N C V S G Y L G R C Q F S D L E W W E
ref|XP_039520437.1|:934-985 N N V V Q S C P S T H D S Y C L Y D G V C F Y F P E M E S Y A C N C V L G Y M G R C Q F S D L E W W E
ref|XP_056328151.1|:963-1014 N N G M Q S C P S T H D S Y C L Y G G V C F Y F P E M E S Y A C N C V L G Y M G R C Q F S D L E W W E
emb|CAK6968295.1|:851-902 S N S V E S C P S S H E S Y C L Y E G I C F Y F P E M E S Y A C N C V S G Y V G R C Q F S D L E W W E
ref|XP_039520436.1|:975-1026 S N V V Q S C P S T H D S Y C L Y D G V C F Y F P E M E S Y A C N C V L G Y M G R C Q F S D L E W W E
ref|XP_069526364.1|:939-990 S N S V E S C P S T H E S Y C L Y G G V C F Y F P E M E S Y A C N C V S G F M G R C Q F S D L E W W E
gb|KAA8588648.1|:998-1049 S N S I E N C P S T H E S Y C L Y G G V C F Y F P E M E S Y A C N C V A G Y V G R C Q F S D L E W W E
ref|XP_062282195.1|:888-939 S N S V E S C P S S H E S Y C L Y E G I C F Y F P E M E S Y A C N C V S G Y V G R C Q F S D L E W W E
ref|XP_058653064.1|:865-916 N N A V Q S C P S T H D S Y C L Y N G V C F Y F P E M E S Y A C N C V L G Y M G R C Q F S D L E W W E
gb|KAF4104848.1|:929-980 N N A V Q S C P S T H D S Y C L Y N G V C F Y F P E M E S Y A C N C V L G Y M G R C Q F S D L E W W E
ref|XP_058653063.1|:907-958 N N A V Q S C P S T H D S Y C L Y N G V C F Y F P E M E S Y A C N C V L G Y M G R C Q F S D L E W W E
ref|XP_032383448.1|:946-997 S N S I E N C P S T H E S Y C L Y G G V C F Y F P E M E S Y A C N C V A G Y V G R C Q F S D L E W W E
ref|XP_041800377.1|:887-938 S N S V E S C P S T H E S Y C L Y G G V C F Y F P E M E S Y A C N C V S G F M G R C Q F S D L E W W E
gb|MBN3319878.1|:1021-1072 N N L I E S C P S S H E T Y C L Y G G V C F Y I P E I G S Y A C N C V K G Y M G R C Q F S D L E W W E
ref|XP_016407911.1|:906-957 N N S V Q S C P S T H D S Y C L Y D G V C F Y F P E M E S Y A C N C V L G Y M G R C Q F S D L E W W E
ref|XP_067312647.1|:862-913 N N V V Q S C P S T H D S Y C L Y D G V C F Y F P E M E S Y A C N C V L G Y M G R C Q F S D L E W W E
ref|XP_05034923.2|:905-956 N N S V Q S C P S T H D S Y C L Y E G V C F Y L P E L E S F A C S C A S G Y M G R C Q F S D L E W W E
ref|XP_016316712.1|:906-957 N N S V Q S C P S T H D S Y C L Y D G V C F Y F P E M E S Y A C N C V L G Y M G R C Q F S D L E W W E
ref|XP_015200773.2|:948-999 N N L I E S C P S S H E T Y C L Y G G V C F Y I P E I G S Y A C N C V K G Y M G R C Q F S D L E W W E
ref|XP_015200772.2|:981-1032 N N L I E S C P S S H E T Y C L Y G G V C F Y I P E I G S Y A C N C V K G Y M G R C Q F S D L E W W E
ref|XP_065128781.1|:949-1000 N N S V Q S C P S T H D S Y C L Y D G V C F Y L P E L E S F A C S C A S G Y M G R C Q F S D L E W W E
ref|XP_016407910.1|:969-1020 N N S V Q S C P S T H D S Y C L Y D G V C F Y F P E M E S Y A C N C V L G Y M G R C Q F S D L E W W E
ref|XP_016316711.1|:969-1020 N N S V Q S C P S T H D S Y C L Y D G V C F Y F P E M E S Y A C N C V L G Y M G R C Q F S D L E W W E
ref|XP_029918660.1|:908-959 S N S I E S C P S S H D S Y C L Y E G I C F Y F P E M E S Y A C N C A S G Y V G R C Q F S D L E W W E
ref|XP_016316709.1|:969-1020 N N S V Q S C P S T H D S Y C L Y D G V C F Y F P E M E S Y A C N C V L G Y M G R C Q F S D L E W W E
ref|XP_016316710.1|:964-1015 N N S V Q S C P S T H D S Y C L Y D G V C F Y F P E M E S Y A C N C V L G Y M G R C Q F S D L E W W E
ref|XP_016407909.1|:964-1015 N N S V Q S C P S T H D S Y C L Y D G V C F Y F P E M E S Y A C N C V L G Y M G R C Q F S D L E W W E
ref|XP_034398892.1|:834-885 S N S V E S C P S S H E S Y C L Y G G V C F Y F P E M E S Y A C N C V S G Y M G R C Q F S D L E W W E
ref|XP_016407908.1|:969-1020 N N S V Q S C P S T H D S Y C L Y D G V C F Y F P E M E S Y A C N C V L G Y M G R C Q F S D L E W W E
gb|KAI3351475.1|:952-1003 S N S V E S C P S S H E S Y C L Y E G V C F Y F P E M E S Y A C N C V S G Y M G R C Q F S D L E W W E
gb|KAK2891091.1|:875-926 N N A V Q S C P S T H D S Y C L Y D G V C F Y F P E M E S Y A C N C V L G Y M G R C Q F S D L E W W E
ref|XP_043112665.1|:907-958 N N A V Q S C P S T H D S Y C L Y D G V C F Y F P E M E S Y A C N C V L G Y M G R C Q F S D L E W W E
gb|KAL1262016.1|:955-1006 N N A V Q S C P S T H D S Y C L Y D G V C F Y F P E M E S Y A C N C V L G Y M G R C Q F S D L E W W E
ref|XP_068182287.1|:929-980 S N S V E R C P S T H E S Y C L Y H G I C F Y F P E M E S Y A C N C V S G Y M G R C Q F S D L E W W D
ref|XP_073676776.1|:970-1021 N N A V Q S C P S T H D S Y C L Y D G V C F Y F P E M E S Y A C N C V L G Y M G R C Q F S D L E W W E
ref|XP_050983116.1|:970-1021 N N A V Q S C P S T H D S Y C L Y D G V C F Y F P E M E S Y A C N C V L G Y M G R C Q F S D L E W W E
ref|XP_068447771.1|:940-991 S N S V Q S C P S S H E S Y C L Y G G V C F Y F P E M E S Y A C N C V F G Y M G R C Q F S D L E W W E
ref|XP_044061862.1|:945-996 S N S V E S C P S T H E S Y C L Y G G V C F Y I P E M E S Y A C N C V L G Y M G R C Q F S D L E W W D
ref|XP_016387980.1|:670-721 N N A V Q S C P S T H D S Y C L Y D G V C F Y F P E M E S Y A C N C V L G Y M G R C Q F S D L E W W E
ref|XP_056117822.1|:973-1024 N N V V Q S C P S T H D S Y C L Y D G V C F Y F P E M E S Y A C N C V L G Y M G R C Q F S D L E W W E
ref|XP_051275250.1|:945-996 S N S V Q T C P S T H E S Y C L Y G G V C F Y F P E M E S Y A C N C V S G Y M G R C Q F S D L E W W D
ref|XP_070819554.1|:905-956 T N S V E S C P S T H E A Y C L Y G G V C F Y F P E M E S Y G C N C V S G Y M G R C Q F S D L E W W E
ref|XP_056626003.1|:973-1024 N N S V K S C P S T H D S Y C L Y E G V C F Y F P E M E S Y A C N C V S G Y L G R C Q F S D L E W W E
ref|XP_044061864.1|:914-965 S N S V E S C P S T H E S Y C L Y G G V C F Y I P E M E S Y A C N C V L G Y M G R C Q F S D L E W W D
ref|XP_020357476.1|:912-963 T N T V E S C P S S H D T Y C L Y E G V C L Y F P E M E S Y A C N C I S G Y M G R C Q F S D L E W W E
ref|XP_035525395.1|:887-938 S N S V Q T C P S T H E S Y C L Y G G V C F Y F P E M E S Y A C N C V S G Y M G R C Q F S D L E W W D
ref|XP_042348829.1|:1153-1204 S N S V E S C P S T H E S Y C L Y G G V C F Y F P E M E S Y A C N C V S G Y M G R C Q F S D L E W W E
ref|XP_042181579.1|:912-963 T N T V E S C P S S H D T Y C L Y E G V C L Y F P E M E S Y A C N C I S G Y M G R C Q F S D L E W W E
ref|XP_073777405.1|:906-956 - N G V Q S C P S T H D S Y C L Y D G V C F Y F P E M E S Y A C N C V L G Y M G R C Q F S D L E W W E
gb|AAQ91603.1|:906-956 - N G V Q S C P S T H D S Y C L Y D G V C F Y F P E M E S Y A C N C V L G Y M G R C Q F S D L E W W E
ref|XP_073777407.1|:905-955 - N G V Q S C P S T H D S Y C L Y D G V C F Y F P E M E S Y A C N C V L G Y M G R C Q F S D L E W W E
ref|XP_073777406.1|:905-955 - N G V Q S C P S T H D S Y C L Y D G V C F Y F P E M E S Y A C N C V L G Y M G R C Q F S D L E W W E
ref|XP_073777408.1|:904-954 - N G V Q S C P S T H D S Y C L Y D G V C F Y F P E M E S Y A C N C V L G Y M G R C Q F S D L E W W E
ref|XP_065815123.1|:934-985 S N S V E S C P S T H E S Y C L Y E G V C F Y F P E M E S Y A C N C V S G Y L G R C Q F S D L E W W E
ref|XP_067454429.1|:893-944 S N S V E S C P S T H E S Y C L Y E G V C F Y F P E M E S Y A C N C V S G Y M G R C Q F S D L E W W E
ref|XP_038555094.1|:946-997 S N S V E S C P S T H E S Y C L Y G G V C F Y F P E M E S Y A C N C V S G Y M G R C Q F S D L E W W E
ref|XP_037635248.1|:888-939 S N S V E S C P S T H E S Y C L Y G G V C F Y F P E M E S Y A C N C V S G Y M G R C Q F S D L E W W E
ref|XP_045885734.1|:946-997 S N S V E S C P S T H E S Y C L Y G G V C F Y F P E M E S Y A C N C V S G Y M G R C Q F S D L E W W E
ref|XP_070769594.1|:944-995 S N S V E S C P S T H E S Y C L Y E G V C F Y F P E M E S Y A C N C V S G Y M G R C Q F S D L E W W E
ref|XP_073777403.1|:968-1018 - N G V Q S C P S T H D S Y C L Y D G V C F Y F P E M E S Y A C N C V L G Y M G R C Q F S D L E W W E
ref|XP_073777404.1|:967-1017 - N G V Q S C P S T H D S Y C L Y D G V C F Y F P E M E S Y A C N C V L G Y M G R C Q F S D L E W W E
ref|XP_060903549.1|:934-985 S N S V E S C P S T H E S Y C L Y E G V C F Y F P E M E S Y A C N C V S G Y L G R C Q F S D L E W W E
gb|KAL0974310.1|:166-216 - N S I E S C P S S H D T Y C L Y E G V C F Y L P E M E S Y A C N C I S G Y M G R C Q Y S D L E W W D
ref|XP_051944898.1|:979-1029 - N T V Q I C P S T H D S Y C L Y E G V C L Y F P E M E S Y A C N C V S G Y L G R C Q F S D L E W W E
ref|XP_060903550.1|:934-985 S N S V E S C P S T H E S Y C L Y E G V C F Y F P E M E S Y A C N C V S G Y L G R C Q F S D L E W W E
ref|XP_042274198.1|:935-986 S N S V E S C P S T H E S Y C L Y E G V C F Y F P E M E S Y A C N C V S G Y M G R C Q F S D L E W W E
ref|XP_050928569.1|:922-973 S N S V E S C P S T H E S Y C L Y E G V C F Y F P E M E S Y A C N C V S G Y M G R C Q F S D L E W W E
gb|KAF7668536.1|:328-379 S N S V E N C P T T H E S Y C L Y G G V C F Y F P E M E S Y A C N C V S G Y M G R C Q F S D L E W W E
ref|XP_045885735.1|:840-891 S N S V E S C P S T H E S Y C L Y G G V C F Y F P E M E S Y A C N C V S G Y M G R C Q F S D L E W W E
gb|KAK6298555.1|:983-1034 T N T V E S C P S S H E T Y C L Y E G V C F Y F P E M E S Y A C N C I A G Y M G R C Q F S D L E W W E
ref|XP_067373871.1|:910-961 S N S V E G C P S T H E S Y C L Y G G V C F Y F P E M E S Y A C N C V T G Y M G R C Q F S D L E W W E
ref|XP_041700777.1|:983-1034 T N T V E S C P S S H E T Y C L Y E G V C F Y F P E M E S Y A C N C I A G Y M G R C Q F S D L E W W E
gb|KAG8003818.1|:846-897 T N S I E R C P S T H E S Y C L Y G G V C F Y F P E M E S Y A C N C A A G Y M G R C Q F S D L E W W E
ref|XP_067373872.1|:897-948 S N S V E G C P S T H E S Y C L Y G G V C F Y F P E M E S Y A C N C V T G Y M G R C Q F S D L E W W E
ref|XP_056295641.1|:830-881 S N S V E S C P S S H E S Y C L Y G G V C F Y F P E M E S Y A C N C V S G Y M G R C Q F S D L E W W D
ref|XP_016308573.1|:965-1016 N N A V Q S C P S T H D S Y C L Y D G V C F Y F P E M E S Y A C N C V L G Y M G R C Q F S D L E W W D
ref|XP_044219177.1|:902-953 S N S V E S C P S T H E S Y C L Y E G V C F Y F P E M E S Y A C N C V S G Y M G R C Q F S D L E W W E
ref|XP_019901200.2|:988-1036 - - - V E S C P S S H D A Y C F Y E G V C F Y L P E M E S Y A C K C I A G Y M G R C Q F S D L E W W E

```



Figure S9: Sequence alignment of the best binder with the top 100 hits retrieved with BLAST. The graph and the colours represent the sequence identity.

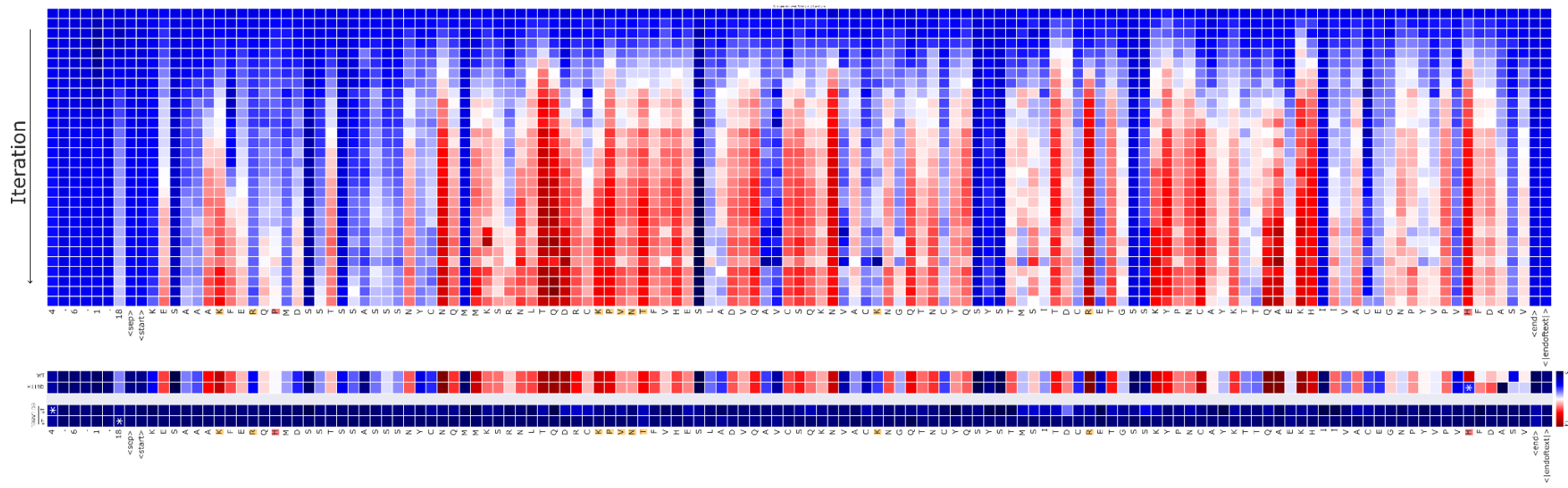


Figure S10: DPO can extract relevant features at the token level. Wild-type sequence for Pancreatic Ribonuclease (EC 4.6.1.18, UniProt: P67926). At the top variation of the reward over the iterations over time for each amino acid. The model identifies key features with higher reward (red color). At the bottom, experiments analyzing single-token variations and their effects compared to the wild-type (WT). Point variation (white asterisks) induce localized changes in the reward, whereas alterations of tokens at the EC label result in a complete drop in the reward across the sequence to zero.

EC number	Objective	Scoring function	Experiments
4.2.1.1	From beta to alpha CA	$(TM_norm_query + align/100)*length_g$ <p>TM_norm_query is the TM score normalized for the query, align is the length of the alignment for the corresponding TM score, and length_g equals the gaussian of the ratio between the WT sequence and the studied sequence centered on 1, as follows: $length_g = \text{math.exp}(-(((len(sequence)/len(ref_seq))-1)**2)/(0.5**2)))$</p>	DPO, self-FT
4.6.1.18	From 10% to 100%	$\text{torch.nn.CosineSimilarity}(ref_clean_emb, target_clean_emb)*length_g$	DPO, self-FT
4.6.1.18	From 10% to 100% (with increased pLDDT)	$\text{torch.nn.CosineSimilarity}(ref_clean_emb, target_clean_emb)*length_g*plddt$	DPO
2.7.11.5	From 0% to 100%	$\text{torch.nn.CosineSimilarity}(ref_clean_emb, target_clean_emb)*length_g$	DPO
5.4.99.5	Increase ProteinMPNN	ProteinMPNN score	DPO
4.2.1.1	Increase ESM1v	ESM1v score	DPO
1.3.3.18	Increase EGF affinity (round 2)	$K_D + length_s + TM_norm_query$ <p>K_D = $(\text{exp}(\max(-\log_{10}(x) - \min_kd, 0)) - 1)*10$ length_s is a score set based on the length of the binder: if between, 80 ad 100 was set to 0.6, more then 100 to 1, otherwise 0.3.</p>	DPO
1.3.3.18	Increase EGF affinity (round 3)	$\text{Expression} * ((K_D + K_on)/2)$	DPO

		Where expression is set to 1, 2 or 3 in case of low, medium or high expression levels respectively. K_on was max() normalized.	
3.2.1.1	Increase activity (SAPI)	cosine_similarity(seq_emb, reference_emb)*plddt*(length_g)	DPO
1.3.3.18	Increase CD80 affinity	score = length_norm * mean [0.80 plddt + i_pTM - 0.8 * pAE_b - 0.8 * pAE_bt - 0.8 * i_pae - 0.5 * pMPNN + 0.3 * shape_complimentary - 0.4 * hydrophobicity - 0.9 * binder_score - 0.3 * interface_dSASA - 0.7 * uns_hydrogens + 0.5 * contact_probs - 0.3 * d_rmsd - 0.5 * binder_sasa + 0.6 * delta_delta_interaction - 0.5 * helicity]	DPO

Table S1: Different scoring functions used in this study.

Table S2: Detailed experimental results for the tested sequences.

Round	K _D (M)	k _{on} (1/Ms)	k _{off} (1/s)	Sequence
1	3.95e-7	2.25e+4	8.89e-3	PENYKSCPPSHDGYCLHGGVCMYISA
	2.61e-7	3.35e+4	8.73e-3	LQAYACNCIQGFVGERCQHSLEWWE
1	4.81e-7	3.55e+4	1.71e-2	PDTIASCSSHESYCLYQGVCFYFPEM
	2.11e-7	8.74e+4	1.84e-2	ESYACNCVSGYMGERCQFSDLQWWELEQ
1	9.10e-7	2.19e+4	1.99e-2	PSTVESCPLSHEGYCLYEGVCFYFPEM
	7.30e-7	-	-	ESYACNCVSGYMGERCQFSDLQWWELEQ
2	3.13e-8	4.53e+4	1.42e-3	SNTVQRCPPSHDAYCLYGGVCFYFPEM
	2.26e-8	4.97e+4	1.12e-3	ESFACKCVKGFVGERCQFSDLQWWE
	2.82e-8	4.27e+4	1.21e-3	
2	4.28e-7	3.61e+4	1.54e-2	NSVERCPSSHDTYCLYGGVCFYFPEM
	2.78e-7	3.55e+4	9.89e-3	FACQCQVNGYLGERCQYADLEWWE
	3.98e-7	3.53e+4	1.40e-2	
2	2.39e-7	2.97e+4	7.10e-3	NSVSDCPASHETFCLNGGTCIYFQLLQ
	2.89e-7	2.10e+4	6.08e-3	EYACRCVKGYMGDRCQFSDLQWWE
	2.29e-7	3.81e+4	8.73e-3	
2	8.23e-7	1.12e+4	9.21e-3	SDCPEAHEGFCLNGGTCIYFVKEYA
	5.06e-7	1.55e+4	7.85e-3	CKCLVGFIGDRCQHRDLRWDL
	5.46e-7	1.39e+4	7.58e-3	
2	2.25e-7	3.92e+4	8.82e-3	PNTVQSCPPSYDSFCLHGGVCIYIPGLEAY
	1.28e-7	3.16e+4	4.04e-3	ACRCVEGYVGERCQFSDLQWWE
	1.90e-7	3.62e+4	6.87e-3	
2	2.44e-7	3.28e+4	7.99e-3	PNSTERCPPSHDSYCLNGGVCIFFSVLQEF
	1.87e-7	4.21e+4	7.89e-3	ACKCLQGYMGERCQHSLEWWE
	1.39e-7	3.34e+4	4.64e-3	
2	8.18e-7	2.15e+4	1.76e-2	SNSVESCSTHDSYCLNGGSCVFFFEIV
	9.35e-7	2.20e+4	2.05e-2	RQFACKCLSGYMGERCQFSDLQWWD
	9.96e-7	1.99e+4	1.98e-2	
2	7.83e-7	1.13e+4	8.87e-3	NSVETCPSTYCLHGGICMFIQAVDRYA
	4.18e-7	1.14e+4	4.77e-3	CKCVVGYVGERCQYRDLRWWSL
	6.02e-7	1.18e+4	7.08e-3	
2	4.04e-7	3.76e+4	1.52e-2	TAPESNYCLNETVIDCPTSHDTFCLYD
	3.59e-7	4.40e+4	1.58e-2	GTCMFIPEMEKYACNLAGFMGDRCQ
	3.88e-7	4.61e+4	1.79e-2	FSDLQWWEWEMQ

Table S3: Hyperparameters used for the training of **ProtRL** unless otherwise specified in the text.

Hyperparameters (DPO)

β	0.01
Seed number	1998
Learning rate	1×10^{-7}
Batch size	5
epochs	5
Train/Test split	0.2
Adams	(0.9, 0.98)
ϵ	1×10^{-8}
Adam decay	0.1